SCIENTIFIC COMMITTEE
FIFTH REGULAR SESSION

10-21 August 2009
Port Vila, Vanuatu

AN UPDATE OF RECENT DEVELOPMENTS AND APPLICATIONS OF THE SEAPODYM MODEL

WCPFC-SC5-2009/EB-WP-10

Patrick Lehodey[1], and Inna Senina[1]

[1] Marine Ecosystems Modeling and Monitoring by Satellites, CLS, Space Oceanography Division, 8-10 rue Hermès, 31520 Ramonville, France

An update of recent developments and applications of the SEAPODYM model

Patrick Lehodey and Inna Senina
Marine Ecosystems Modeling and Monitoring by Satellites

CLS, Space Oceanography Division
8-10 rue Hermès, 31520 Ramonville, France
PLehodey@cls.fr, ISenina@cls.fr

Foreword

SEAPODYM is a model developed initially for investigating spatial tuna population dynamics, under the influence of both fishing and environmental effects. This modelling effort started in 1995 at the Secretariat of the Pacific Community in Noumea, New Caledonia, under two consecutive EU-funded projects: SPR-TRAMP (1995-2000) and PROCFISH (2002-2005). The model development also benefited of a grant from the PFRP (Pelagic Fisheries Research Program) of the University of Hawaii, allowing the implementation of irregular grids and initiating the work for parameter optimization (2004-05). Since 2006, the development has continued within the MEMMS section (Marine Ecosystem Modeling and Monitoring by Satellites) of the Spatial Oceanography Division of CLS, a subsidiary of the French CNES and IFREMER Institutes. An enhanced version of the model (SEAPODYM.v2.0) has been achieved last year (Lehodey et al 2008; Senina et al. 2008; Lehodey et al. 2008b) and the user's manual updated (Lehody and Senina 2009).

Collaboration with SPC and PFRP continues, with funding support from the EU-funded SPC project SCIFISH, and a second PFRP grant (*Climate and Fishing Impacts on the Spatial Population Dynamics of Tunas*: project no. 657425). Another project to apply SEAPODYM to Pacific swordfish has been initiated recently at the NOAA-NMFS Pacific Islands Fisheries Science Center, in Hawaii. The model is also used to investigate the movement and habitats of Atlantic bluefin tuna under a one-year project funded by the Large Pelagic Research Center of the University of New Hampshire, with the objective of using archival tagging data assimilation for parameter optimization (Lehodey et al., 2009).

Introduction

Using the enhanced version of the model SEAPODYM.v2.0, our first key objective is to produce an envelope of prediction of biomass for the main Pacific tuna species (skipjack, yellowfin, bigeye and albacore) for the last 50 years, based on different environmental forcing data sets. The approach is using data assimilation techniques (Fig. 1), like in other models used for stock assessment studies (e.g., MULTIFAN-CL, A-SCALA, …), however, it is different as it is an explicit spatial model driven by oceanic environmental variables. Therefore, fishing data (catch, effort and size frequencies) are spatially-

disaggregated, typically at monthly 1 to 5 degree square resolution for catch and effort, and quarterly 5 to 20 degree square resolution or more for size frequency data (Senina et al 2008).

In SEAPODYM, the dynamics of tuna populations are driven by environmental forcing (temperature, currents, dissolved oxygen, euphotic depth, and primary production) and prey (micronekton) distribution that can be predicted from coupled physical-biogeochemical models. Because the model is driven by the bio-physical environment of the ecosystem, it was possible to reduce the number of parameters that describe the complete spatially-explicit population dynamics of a species to a small number (17) relative to the number of variables described in the model (see appendix 1). In addition, the model requires 3 parameters for each fishery to define catchability and selectivity. These parameters are also estimated through the optimization approach.

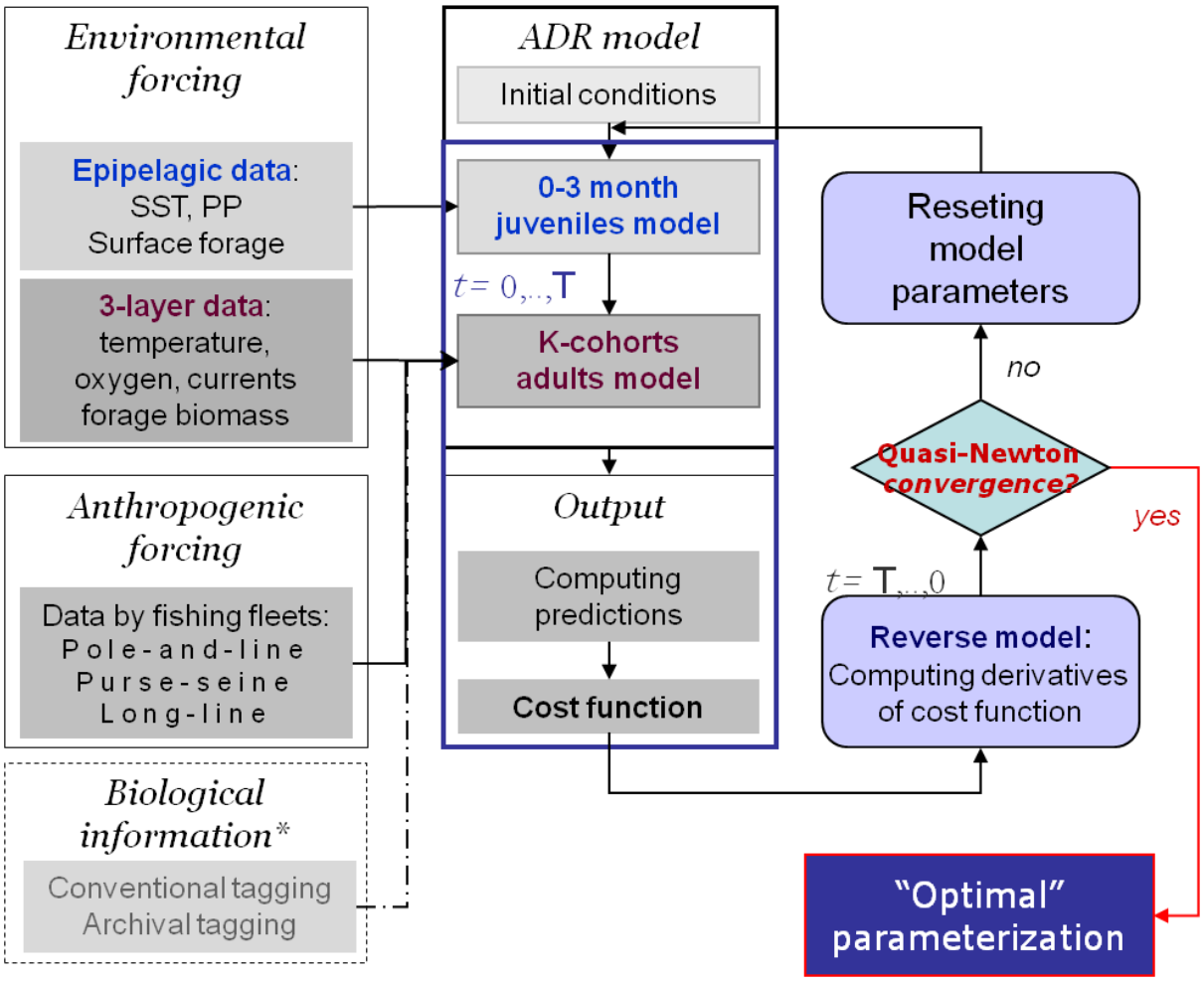

Figure 1. General scheme of the SEAPODYM model with optimization approach.

*Preliminary work has been initiated for including tagging data into the optimization process.

However, the counter-part of this parsimonious modeling approach is its sensitivity to the quality of the forcing data set. Though coupled physical-biogeochemical models predict relatively good basin scale

variability of the environment, they are far to reproduce the exact oceanic conditions, and each model configuration has its own strength and weak points. Thus, it becomes necessary to test different model forcings to produce an envelope of prediction that will be more reliable than any single simulation. While we are still running a large number of optimization experiments to obtain this simulation ensemble, this report presents a summary of the key results for each tuna species obtained with either one or two model configuration outputs. Stock assessment results are compared to those of MULTIFAN-CL, and the spatial population dynamics are presented highlighting the effect of seasonal and interannual environmental variability.

Physical-biogeochemical forcing

The first environmental forcing used for optimization experiments was the ESSIC configuration (Univ. of Maryland) with a first vertical definition of 3 layers between 0-100m, 100-400m and 400-1000m (Lehodey et al., 2008, Senina et al. 2008). Here we present new results using two other configurations. They have the same physical (ORCA2) and biogeochemical (PISCES) models but used two different atmospheric forcing: NCEP and ERA40. Also, a different definition of vertical layers was used with epipelagic layer between 0 and one euphotic depth (Z_{eu}), mesopelagic layer between 1 and $3Z_{eu}$ and bathypelagic layer between $3Z_{eu}$ and 1000m. A third environmental forcing based on the Community Climate System Model (CCSM) has been recently obtained through a contract under the PFRP project with the National Center for Atmospheric Research (NCAR) and will be used in the ensemble simulation.

ORCA2 is the standard configuration of the ocean general circulation model OPA (Version 9.0) for the global ocean (http://www.nemo-ocean.eu/).

ESSIC is a biogeochemical model developed at the Earth System Science Interdisciplinary Center (Univ. Maryland, USA). It is based on the sigma-coordinate general circulation model of Gent and Cane (1989) as further developed by Chen et al (1994) and Murtugudde et al. (1996), and the ecosystem model of Leonard et al. (1999).

PISCES (Pelagic Interaction Scheme for Carbon and Ecosystem Studies; Aumont and Bopp, 2006) is derived from the Hamburg Model of Carbon Cycle, HAMOCC3.1 (Six and Maier-Reimer, 1996) and HAMOCC5 (Aumont et al. 2003). This model describes the marine biogeochemical cycles of carbon and of the main nutrients (N, P, Si and Fe) which limit phytoplankton growth. Description of the model behavior and validation to observations are found in Gorgues et al. (2005), Bopp et al. (2005) and Aumont and Bopp (2006).

NCEP: The NCEP-NCAR reanalysis provides 50-year record of global analyses of atmospheric fields based on the recovery of land surface, ship, rawinsonde, pibal, aircraft, satellite, and other data; quality controlling and assimilating these data with a data assimilation system that is kept unchanged over the reanalysis period. This eliminates perceived climate jumps associated with changes in the data assimilation system. These atmospheric fields are used to drive ocean circulation models.
http://www.cgd.ucar.edu/cas/guide/Data/ncep-ncar_reanalysis.html

ERA40: This atmospheric reanalysis is produced by the ECMWF and covers the period from mid-1957 to 2001 (Uppala et al., 2005). See: http://www.ecmwf.int/research/era/do/get/era-40.

CCSM: The primary goal of the Community Climate System Model (CCSM) project is to develop a state-of-the-art climate model and to use it to perform the best possible science to understand climate variability and global change. See http://www.ccsm.ucar.edu/. We will use a reanalysis of the World Ocean State (physics and biogeochemistry) deduced from this Climate System Model (CCSM) for the period Jan 1st 1950 – Dec 31 2005. This reanalysis has a variable horizontal and vertical resolution ranging from 0.6 deg. at the equator down to 3 deg. in the highest latitude. The ocean is similar to the version described in Yeager et al. (2006), and the ecosystem is similar to the version in Moore et al. (2004). A spin-up of 500 yr was used to insure stability and a net ocean heat uptake of less 0.1 W/m2. The run has then been continued with two 55 yr cycles of interannual forcing (CORE II, yrs 1949-2004). A final, 3rd, cycle was added and all model output was saved every 5 days.

Table 1 – Ocean model configurations used for optimization experiments with four Pacific tuna species at the date of June 1st 2009.

	SKJ	YFT	BET	SP Alb.
Configuration ESSIC (1948-2004; 2deg; monthly)	X		X	
Configuration NCEP-ORCA2- PISCES (1948-2003; 2deg; monthly)		X		X
Configuration ERA40-ORCA2- PISCES (1955-2001; 2deg; monthly)		X		X
Configuration CCSM (1950-2003; ~1deg; 5d)	In preparation			
Periods used for optimization	1980-2000	1983-2004	1984-1999	(1) 1958-1978 (2) 1980-2001
Fishing events used in optimization (catch-effort / size frequencies)	174,221 / 1,571	352,160 / 9,534	362,424 / 1,492	(1) 23,751 / 4,291 (2) 39,601 / 3,475
Hindcast and validation	1950-2004		1978-2004	
Nb fisheries (cf. appendix 2)	WCPO: 4 EPO: 2 PS	WCPO: 15 EPO: 3 PS & 2 LL (MFCL)	26 (MFCL)	12 LL

Model summary

SEAPODYM is a model developed initially for investigating spatial tuna population dynamics, under the influence of both fishing and environmental effects. The model is based on advection-diffusion-reaction equations. The main features of this model are i) forcing by environmental data (temperature, currents, primary production and dissolved oxygen concentration), ii) prediction of both temporal and spatial distribution of mid-trophic (micronektonic tuna forage) functional groups, iii) prediction of both temporal and spatial distribution of age-structured predator (tuna) populations, iv) prediction of total catch and size frequency of catch by fleet when fishing data (catch and effort) are available, and v) parameter optimization based on fishing data assimilation techniques.

A recent enhanced version (Lehodey et al., 2008) has been developed that includes a better definition of habitat indices, movements, and accessibility of tuna and tuna-like predators to different vertically migrant and non-migrant micronekton functional groups (Lehodey et al., *in press*). These groups are represented in a three layer vertical environment delineated using predicted euphotic depth that is used to achieve a more realistic vertical structure. Thus, the epipelagic layer is between surface and 1x euphotic depth, the mesopelagic layer between 1x and 3x the euphotic depth and the bathypelagic layer between 3x the euphotic depth and 1000 m. Temperature, zonal (u) and meridional (v) currents and dissolved oxygen predicted from ocean physical-biogeochemical simulations are averaged following this definition of layers while total primary production is integrated over the entire vertical layer.

The model is parameterized through assimilation of commercial fisheries data, and optimization is carried out using maximum likelihood estimation approach (Senina et al., 2008). For parameter optimization, we implemented adjoint methodology to obtain an exact, analytical evaluation of the likelihood gradient. The approach to select the "best parameter estimate" is based on a series of computer experiments in order i) to determine model sensitivity with respect to variable parameters and, hence, investigate their observability, ii) to estimate observable parameters and their errors, and iii) to justify the reliability of found solution.
The uncertainties of parameter estimates are provided by the diagonal elements of error-covariance matrix calculated as the inverse of the Hessian.

For skipjack, yellowfin and bigeye, the model domain covers the Pacific Basin at a spatial resolution of 2 deg x 2deg and a monthly time resolution. We conducted a series of simulations with optimal parameters estimated from actual fishing data for the recent period (Table 1). To evaluate the capacity of the model to capture the essential features of the dynamic of the tuna species, we carried out hindcast simulations back to the early 1960s, i.e., the beginning of the industrial fishing, with the fixed "best-parameterization" achieved from optimization experiments and compared predicted catches conditioned on the observed fishing effort and observed catches. For south Pacific albacore a sub-domain was extracted to represent the south Pacific basin between 5°N and 55°S.

Population structure

The model simulates tuna age-structured populations with one length and one weight coefficient by cohort obtained from independent studies (Hampton et al., 2006, Langley et al., 2007; Hoyle et al., 2008). Different life stages are considered: larvae, juveniles and (immature and mature) adults. The age structure is defined with one monthly age class for larvae and two monthly age classes for juveniles, and then age classes can be defined by quarter, half-year or one-year according to the lifespan of the species (see

appendix 1). After juvenile phase, fish become autonomous, i.e., they have their own movement (linked to their size and feeding habitat) in addition to be transported by oceanic currents. Fish are considered immature until pre-defined age at first maturity and mature after this age, i.e., contributing to the spawning biomass and with their displacements controlled by a seasonal switch between feeding and spawning habitat outside of the equatorial region. The last age class is a "plus class" where all oldest individuals are accumulated. All temporal dynamics are computed at the time step of the simulation, i.e., one month in the present case (see previous cited references for more details).

Fisheries

A stratification of fisheries has been defined for each tuna species in collaboration with colleagues of the Oceanic fisheries Programme (see appendix 2). These simulations were conducted without detailed size frequency data of purse seine and longline fisheries in the EPO. Given the importance of this region for yellowfin and bigeye in particular, it would be really helpful to run further optimization experiments with more detailed size and catch distribution in this region.

The total amount of fishing data events used for model calibration is very high (table 1), but nevertheless optimization experiments have shown a strong sensitivity to limited but obviously aberrant fishing data. Lack of convergence in the optimization process frequently allowed to quickly identify a problem in the fishing dataset, e.g., obvious mistakes in latitude or longitude, switch between catch and effort, aberrant effort or catch, catch with zero effort… etc. Then, it was necessary to exclude from the optimization procedure some fisheries, either because of their lack of accuracy (e.g., Philippine and Indonesia fisheries) or because of gradual change in the fishing strategy and target species (e.g., Japanese longline in the case of albacore). However, the catch by these fisheries is accounted for the fishing mortality.

Results

Skipjack

Results concerning optimization experiments of Pacific skipjack using ESSIC forcing have been published in Senina et al. (2008). Key results are:

- The dynamics predicted by SEAPODYM are generally in agreement with the statistical length-based stock assessment model, MULTIFAN-CL, (Fig. 3), with the correlation R2 = 0.46 between the two biomass estimates.
- SEAPODYM predictions suggest much more moderate (in amplitude) variations in skipjack stock, likely driven also by underestimated range of variability predicted by the biophysical coupled model.
- SEAPODYM predicts the east-west movement of skipjack in the warmpool as observed from catch and tagging data (Lehodey et al., 1997).
- Dynamics of the population biomass predicted by SEAPODYM and MULTIFAN-CL differ substantially during 1978–1982 and 1992–1997 periods. These two periods correspond to post-El Niño ecosystem conditions which are known to be favorable for skipjack recruitment (Lehodey et al., 2003) through expansion of the skipjack spawning grounds and then, bringing more accessible forage to the western–central Pacific region.

- Comparison of predicted biomass time series of young tuna and the Southern Oscillation Index (SOI) shows direct relationship between ENSO events and changes in the population dynamics (Fig. 3).
- The general trend in abundance of the adult stock is predictable 8 months in advance simply using the SOI (Fig. 4).

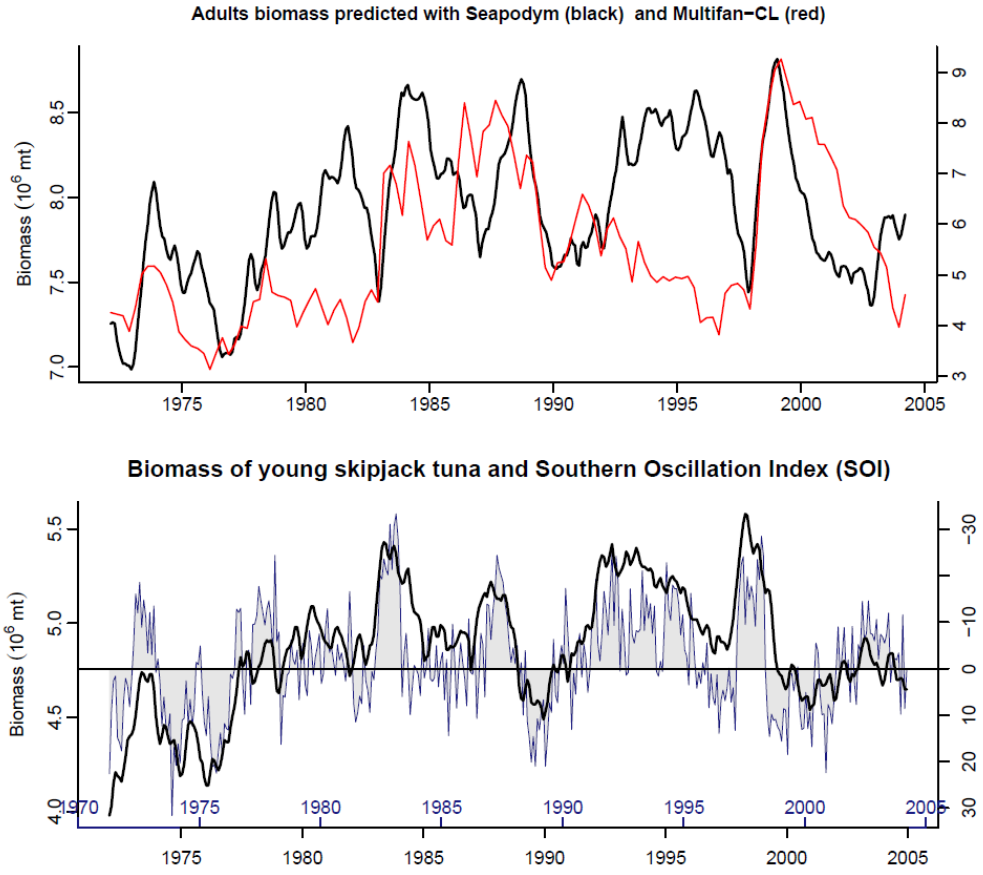

Figure 3. **Skipjack** (from Senina et al. 2008). Upper plot shows comparison of predicted biomass of skipjack in WCPO area (all MFCL regions) by SEAPODYM and MULTIFAN-CL models, R^2=0.46. Parameterization achieved was used to simulate population dynamics for wider time period, starting from 1972. Lower plot shows biomass of young skipjack tuna (sum of ages from 3 month to 3 quarter) and eight month lagged Southern Oscillation Index (notice that y axis is inverted) as an indicator of El-Nino event.

Note that the US Climate Prediction Center has released a recent ENSO bulletin indicating that "Current observations and dynamical model forecasts indicate El Niño conditions will continue to intensify and are expected to last through Northern Hemisphere winter 2009-10". If this event is confirmed, and based on the relationship identified above, the Pacific skipjack biomass should increase in 2010, following the decrease that likely occurred during the past year.

Bigeye

The parameter optimization of the SEAPODYM model for bigeye tuna was conducted using historical fishing data over the period 1985-2004 with the ESSIC forcing. Fishing data included spatially-disaggregated monthly catch data for 4 purse-seine fisheries and 2 pole-and-line fisheries at an original resolution of 1x1 deg. and 15 longline fisheries (5x5 deg. resolution) with quarterly length frequency data associated with each fishery over the historical fishing period (data provided by the Secretariat of the Pacific Community and Inter-American Tropical Tuna Commission).

Final estimates of the parameters are presented in appendix 1. The experiments showed a generally good fit to the fishing data both for monthly catch time series and length frequency distribution of catch, and parameter estimates are biologically plausible. Examples of spatial distribution of predicted biomass of young and adults are presented in Fig. 4 for two typical periods marked by El Niño and La Niña phases. It should be noted that for this environmental forcing only a monthly climatology was available for the oxygen, likely producing bias in the definition of the habitat, especially in the EPO where dissolved oxygen concentration can be a limiting factor.

Optimal spawning temperature is estimated to be 26.2^{o}C with narrow standard deviation of the Gaussian function (0.8 ^{o}C). This range of temperature values corresponds typically to those observed at sea for mature and spawning bigeye tuna (e.g., Schaeffer 2005). Optimal habitat temperature of the oldest cohort was estimated to be 13^{o}C with 2.16^{o}C standard deviation. The resulting temperature habitat by age is shown on Fig. 5. Physiological experiments suggest that bigeye tuna are more tolerant to low ambient oxygen than other tuna species (Brill 1994; Lowe et al. 2000). The estimated oxygen threshold parameter obtained for this species (0.46 ml/l) is effectively the lowest compared to other tuna species.

Natural mortality rates are the most difficult parameters to estimate in population dynamic models. For bigeye, it was estimated by analysis of catch-at-age data for the longline fishery (i.e., for large fish) to be 0.03 month^{-1} (Suda and Kume, 1967). Other estimates obtained from analyses of tagging data in the western Pacific Ocean range from 0.56 month^{-1} for small fish (20-40 cm) to 0.04 month^{-1} for fish of 60-110 cm (Hampton et al., 1998). In SEAPODYM, natural mortality is defined by the combination of two functions (Fig. 5) allowing the mortality rates to vary with age (size) but also spatially and temporally within a range of values related to the habitat index. Parameters estimated for the functions in both experiments produce reasonable natural mortality coefficient-at-age compared to other studies (Fig. 5) but with higher values for the oldest cohorts. The parameter β_s that constrains this part of the curve however is the most difficult to estimate by the model.

The asymptote value of the Beverton-Holt relationship, R_s is also difficult to estimate in population dynamics models. The SEAPODYM optimizer estimated R_s with relatively large uncertainty. This parameter defines the number of larvae released in each cell of the grid in relation with spawning biomass and weighted by the spawning index. This value, together with the mortality rates, determines the total level of the population.

Larvae density 1st semester 1998	Larvae density 1st semester 1999

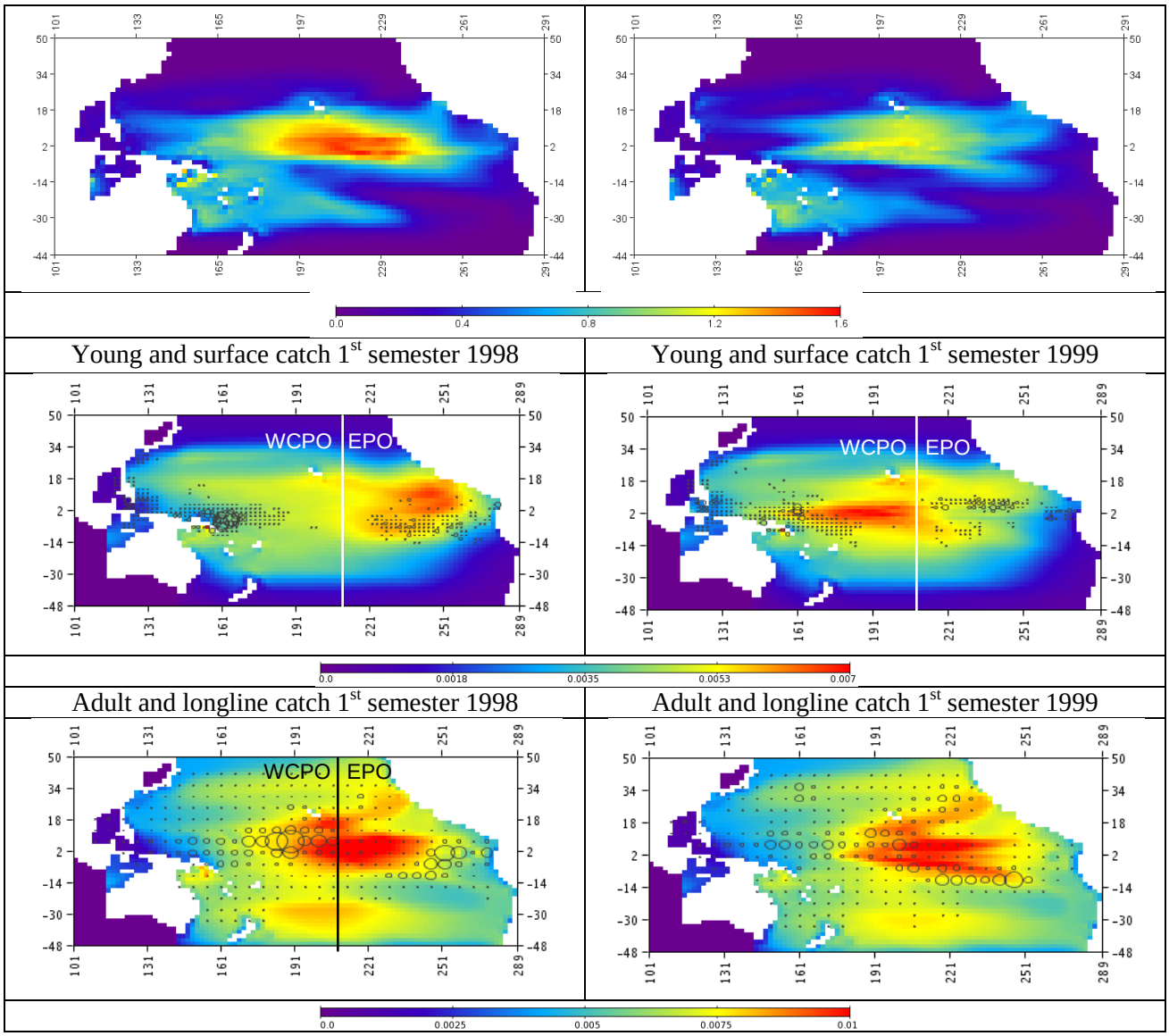

Figure 4: **Bigeye tuna**. Average distribution for the 1st semester 1998 (El Niño phase) and 1st semester 1999 (La Niña phase) of larvae density (top), total catch (proportional to circles) observed in surface and longline fisheries distribution superimposed on predicted young (middle) and adult (bottom) fish biomass ($g \cdot m^{-2}$) respectively.

Estimated diffusion (D_{max}) gives diffusion rates ranging from 560 $nmi^2 day^{-1}$ (on average) for young cohorts to 2830 nmi^2 day^{-1} for adult fish. Parameter of directed movement (along positive gradient of habitat index) was estimated to be 0.32 body lengths per second. Note that movement velocities are computed as the sum of directed (behavioural) and passive (currents) components.

Using this first optimal parameterization, we ran the model starting in 1960 with initial conditions generated by a spin-up simulation and excluding the first 5 years from our evaluation to reduce the effect of initial conditions. Figure 6 compares the estimates of adult bigeye biomass in western-central (WCPO)

and eastern (EPO) Pacific for both the optimization period and hindcast period with independent series from stock assessment studies using the model MULTIFAN-CL (Hampton and Fournier 2001; Hampton et al. 2006; Sibert et al. 2006). Despite the large uncertainty on the R_s parameter, the final biomass predicted by SEAPODYM is of the same order as that obtained by MULTIFAN-CL. The latter however, showed a higher variability and a stronger decreasing slope in the initial period of the industrial fishery (1965-75).

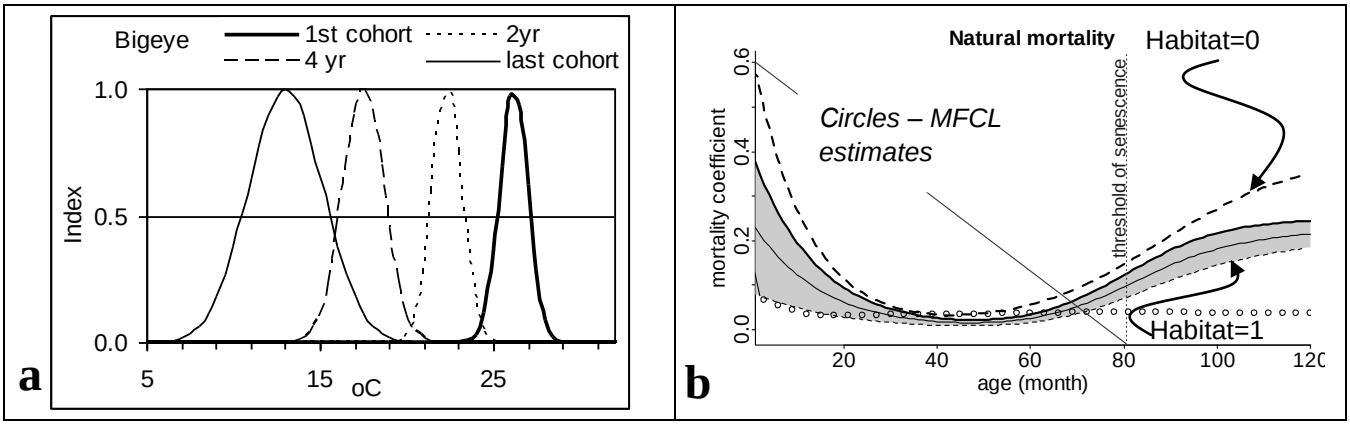

Figure 5: Representation of the thermal habitat and natural mortality of Pacific bigeye tuna obtained through parameter optimization process based on the ESSIC forcing data set and fishing data for 1985-2004. a) Change in habitat temperature by cohort; b) Mortality coefficient-at-age (month^{-1}) with range of variability linked to habitat values and estimates from MULTIFAN-CL (circles).

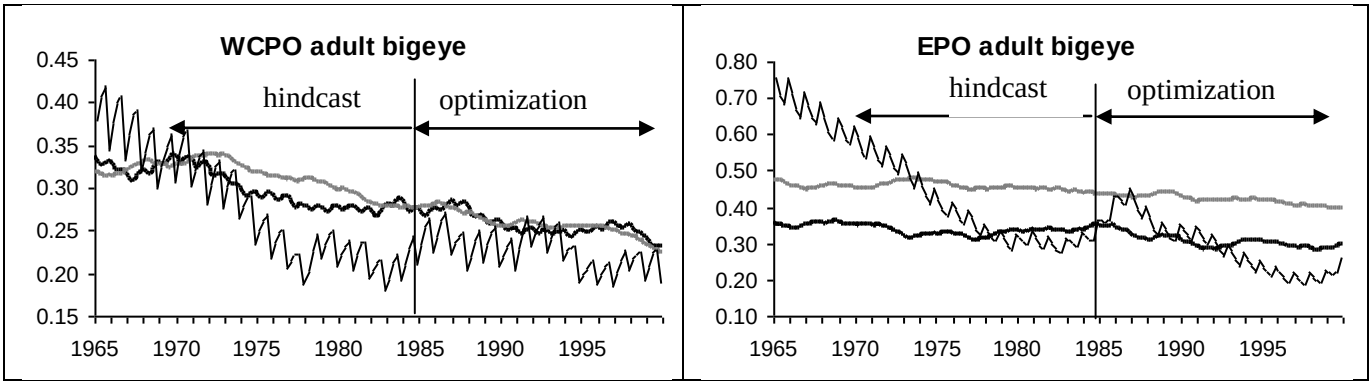

Figure 6: Biomass trends (million tonnes) in Pacific bigeye tuna population predicted in WCPO and EPO with optimization (1985-2004) and hindcast prediction to 1965 for the two experiments based on ESSIC (black thick line) and IPSL (grey line) forcing fields. The trends for adults are compared to estimates (thin black line) from stock-assessment model MULTIFAN-CL (Hampton et al. 2006, Sibert et al. 2006).

Yellowfin

The parameter optimization of the SEAPODYM model for yellowfin tuna was conducted using historical fishing data (Fig. 7; see definition of fisheries in appendix 2) over the period 1983-2004 with two different environmental data sets produced with the same model configuration (ORCA2-PISCES) but under two different atmospheric forcing reanalyses: NCEP and ERA40. Despite that both configurations have the same ocean and biogeochemical models, the predictions under different atmospheric reanalyses lead to substantial differences in ocean conditions. Comparison between the two forcing wind stress fields shows that ERA40 has stronger wind stress in the tropical zone than NCEP. This leads to a stronger equatorial upwelling in the ORCA2-ERA40 configuration. Also, due to coarse resolution, both simulations underestimate the intensity of oceanic circulation in the most dynamical oceanic areas: Kuroshio, East equatorial Pacific.

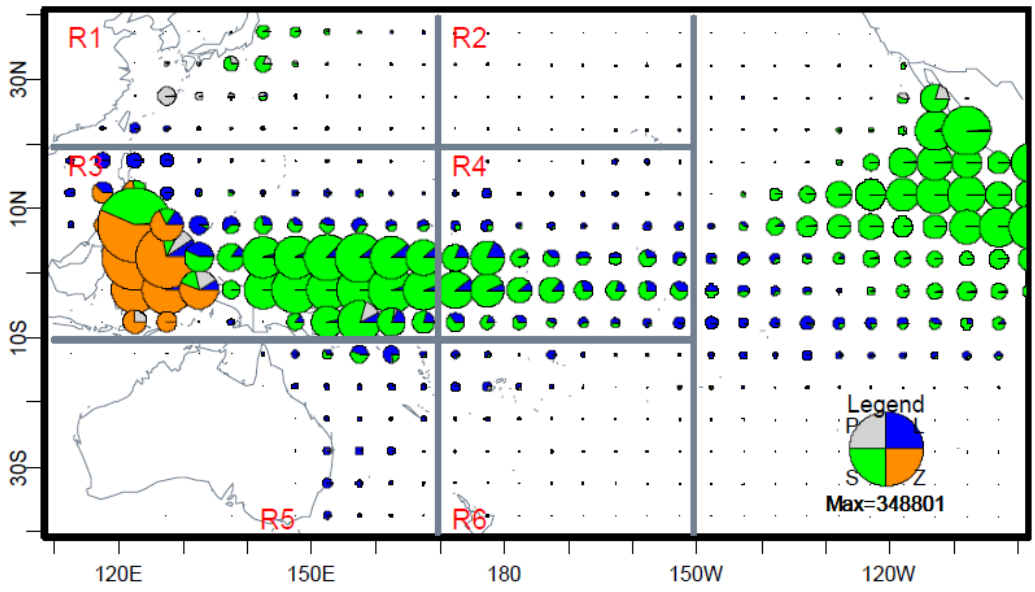

Figure 7 (from Langley et al., 2007). Distribution of cumulative yellowfin catch from 1990−2005 by 5 degree squares of latitude and longitude and fishing gear, with MFCL regions (grey lines). Longline (blue), purse-seine (green), pole-and-line (grey) and other (dark orange).

These first optimization experiments for yellowfin have shown that parameter calibration is sensitive to the oceanic environment predicted by coupled physical-biogeochemical models. For example, despite very close optimal spawning temperature habitat obtained in both configurations, i.e., 25.98°C and 26.53°C for NCEP and ERA40 forcing respectively, the resulting spatial distributions of larvae are quite different (Fig. 8). The results are also sensitive to the length of the time period used for parameter optimization, the initial conditions, and to the quality and coverage of fishing data. A stratification of fishing data into homogeneous fisheries is critical. These simulation experiments did not included detailed size frequency data for the EPO, a key area for yellowfin, and thus need to be updated as we received these data recently.

In both configurations the model converged with a reasonable fit to fishing data (Appendix 3). However, there is still inconsistency in the parameter estimates, and for some fisheries (catch or size frequency).
The comparison between MULTIFAN-CL and SEAPODYM estimates showed higher total biomass predicted by SEAPODYM, but comparison by MFCL region indicated important differences.

For adult yellowfin, SEAPODYM predicted much higher biomass in the sub-tropical regions (1, 2, 5, and 6) than MULTIFAN-CL (Fig. 9), but similar (area 4) or even less (area 3) biomass levels in the tropical region which is the core habitat of the species. Sub-tropical regions correspond to areas of intense mesoscale activity (Kuroshio and Australian current) potentially leading to high but concentrated catch. Given the coarse resolution of the model configuration used here, it is likely that SEAPODYM tends to increase biomass and diffusion in these regions to fit the observed catch.

The contrast is still higher when considering total biomass, i.e. including the immature fish that are mainly caught by purse seiners (Fig. 10). Here, SEAPODYM can predict a good fit to catch by surface fisheries (appendix 3: purse seine (S) and pole-and-line (P) fisheries) in the tropical regions (3 and 4) with a lower biomass than predicted by MULTIFAN-CL.

Parameterization experiments still need to be continued with a careful check of fishing data where there is a difficulty to obtain a good fit to observation, and with the additional detailed data for the EPO. New model configurations with higher resolution and more realistic mesoscale features should be tested to analyze the impact on subtropical regions.

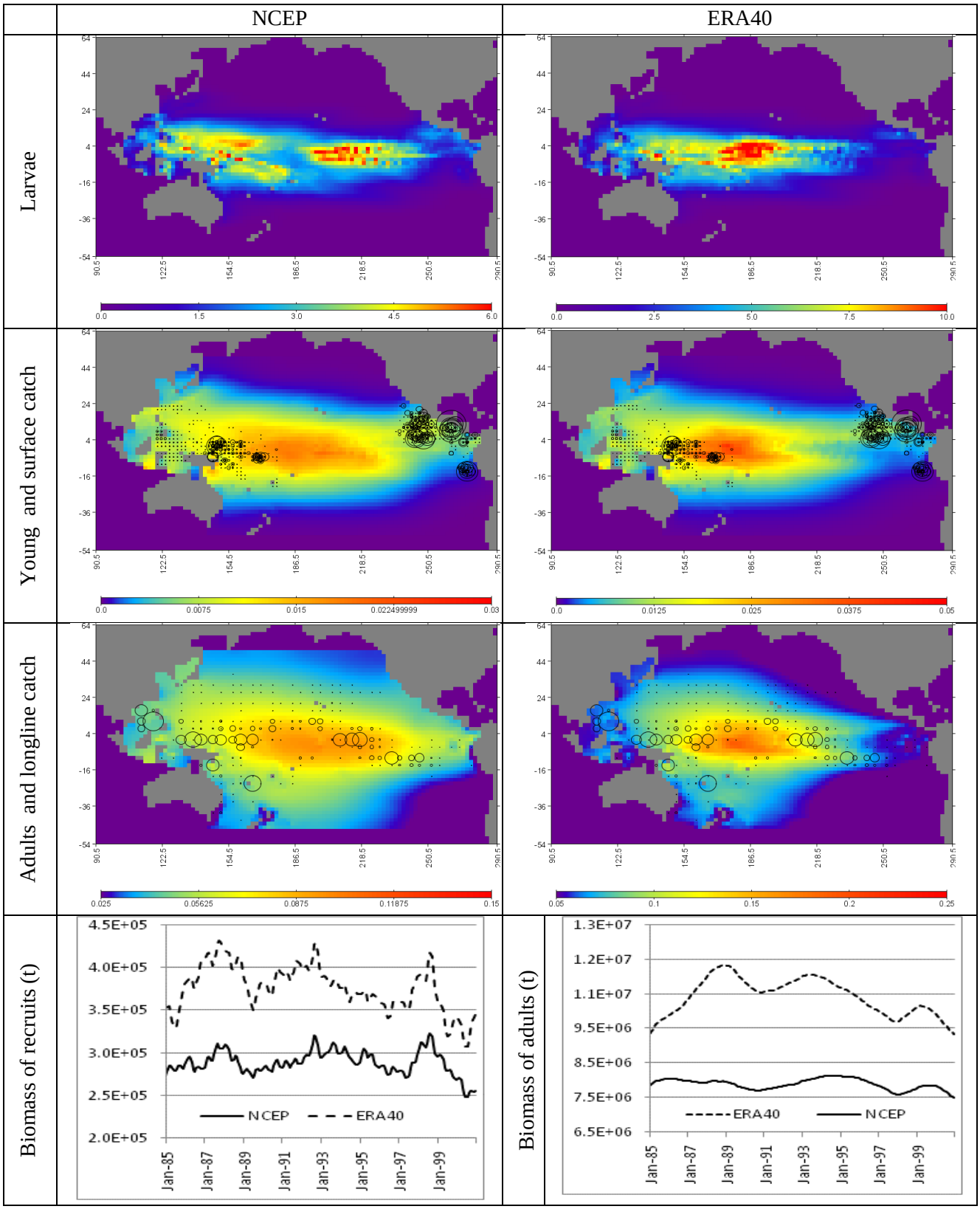

Fig. 8. Biomass estimates of Pacific yellowfin tuna recruits and adults using two different physical-biogeochemical oceanic environments: NCEP-ORCA2-PISCES and ERA40-ORCA2-PISCES.

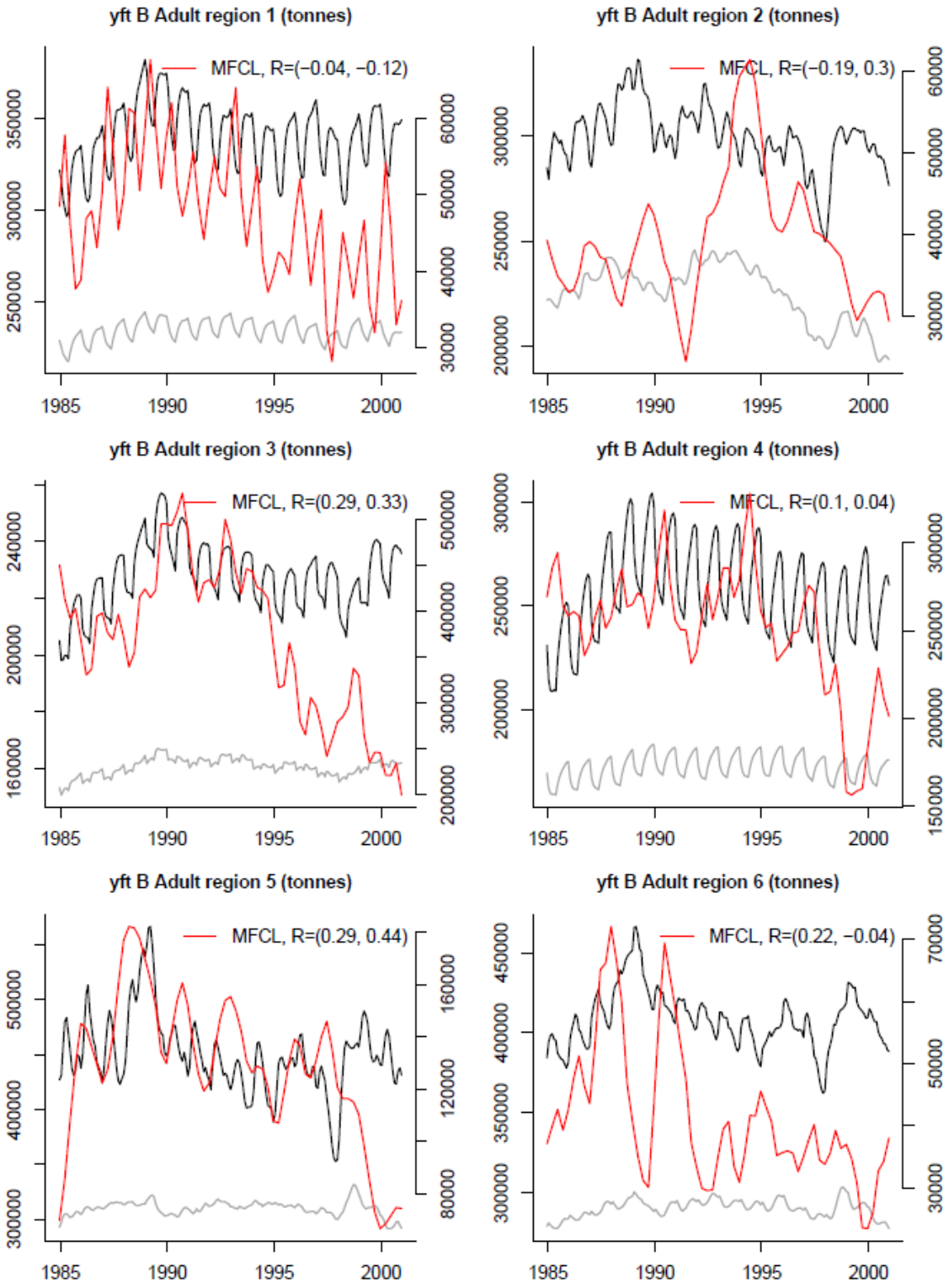

Figure 9. Comparison of adult biomass (t) of yellowfin estimated by SEAPODYM (black and grey, right axis) and MFCL (red, left axis) for each region used by MULTIFAN-CL (Fig. 7).

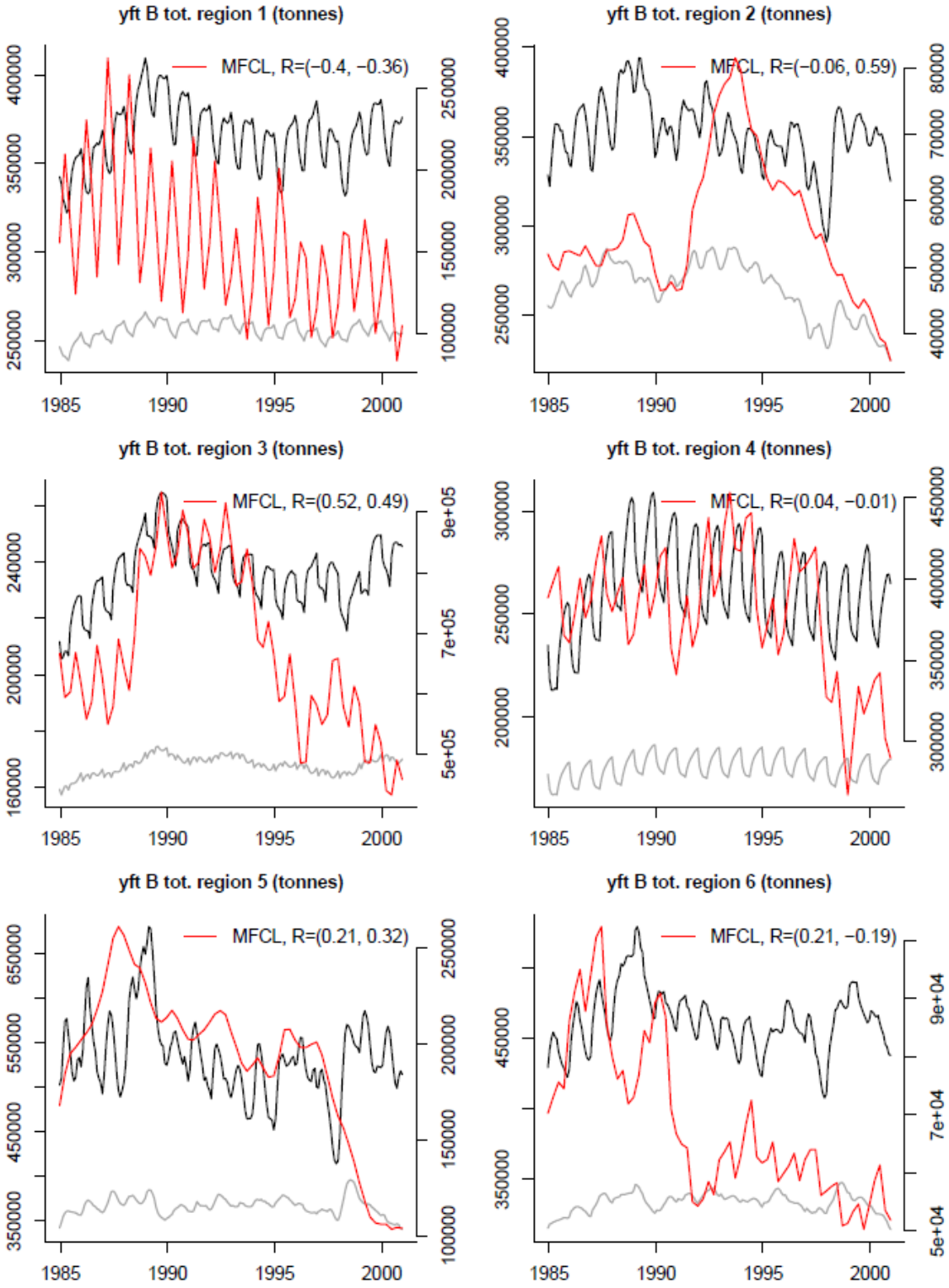

Figure 10. Comparison of total biomass (t) of yellowfin estimated by SEAPODYM (black and grey, right axis) and MFCL (red, left axis) for each region used by MULTIFAN-CL (Fig. 7).

South Pacific Albacore

Due to the long lifespan of albacore and the relatively short time series used, as well as limited information (fishing data) for juvenile fish, the model calibration for this species is particularly sensitive to initial conditions. We therefore conducted a preliminary optimization experiment for the period 1958-1978 to define initial condition used to run the 1980-2001 experiment. The parameter optimization of the SEAPODYM model for south Pacific albacore tuna was conducted using historical fishing data as defined by fisheries in appendix 2). First simulation experiments using NCEP configuration were including 8 longline fisheries: domestic fisheries of Fiji and New Caledonia, Samoa, American Samoa, Tonga and French Polynesia were combined together (L5). But in the second series of simulations using ERA40, it was decided to split the Japanese fishery in two since fishing strategy are different in tropical (north of 25S) and sub-tropical and temperate (south of 25S) regions. The Samoan and American Samoan fishery were combined in a separate domestic longline fishery (LL 11).

The results from these simulations are still preliminary and there is still inconsistency in several parameter estimates between the different configurations. In particular the NCEP configuration leads to high optimal spawning temperature (28.9°C), while ERA40 configuration gives more plausible value (25.56°C), according to the knowledge on this species. In both cases, the optimization approach suggests high sensitivity to dissolved oxygen concentration with a threshold value between 3-4 $ml \cdot l^{-1}$.

In both configurations the model can converge with a reasonable fit to fishing data (Appendix 4). The redefinition of Japanese longline fishery in the ERA40 configuration allowed a substantial improvement in the likelihood and the fit to data (see appendix 4, LL1 with NCEP configuration vs LL1 and LL12 in ER40 configuration) both for catch and size frequency, as albacore catch in the tropical region (L12) have larger size than in the temperate fishery (L1).

A natural separation of the south Pacific albacore population emerged from these simulations (Fig. 11), due to constraints associated to the definition of thermal, feeding and spawning habitats. The predicted low tolerance to hypoxic waters in particular produced an unfavorable habitat in the eastern equatorial Pacific. The model predicted a clear seasonal migration pattern of adult fish between the feeding grounds in the southern convergence mostly favorable during austral summer (January to May) and the spawning grounds in warmer waters of the southern tropical area (October to December).

Initial conditions are critical to estimate the absolute biomass. In the first experiment based on NCEP forcing, the model predicted a high biomass of young fish (Fig. 12) as the optimizer tried to fit the size distribution of catch for the whole Japanese longline fishery including both small and large fish. In the second experiment using ERA40 and two separate Japanese tropical and temperate longline fisheries the model predicted a much lower initial biomass of young fish but that finally led to higher biomass of adults than in the NCEP experiment. Both estimates tend to converge in the end of the time series (Fig. 13), but are still an order of magnitude higher than the MLTIFAN-CL estimate (Fig 13).

Optimization experiments with NCEP configuration will be therefore updated using this revision in the definition of fisheries.

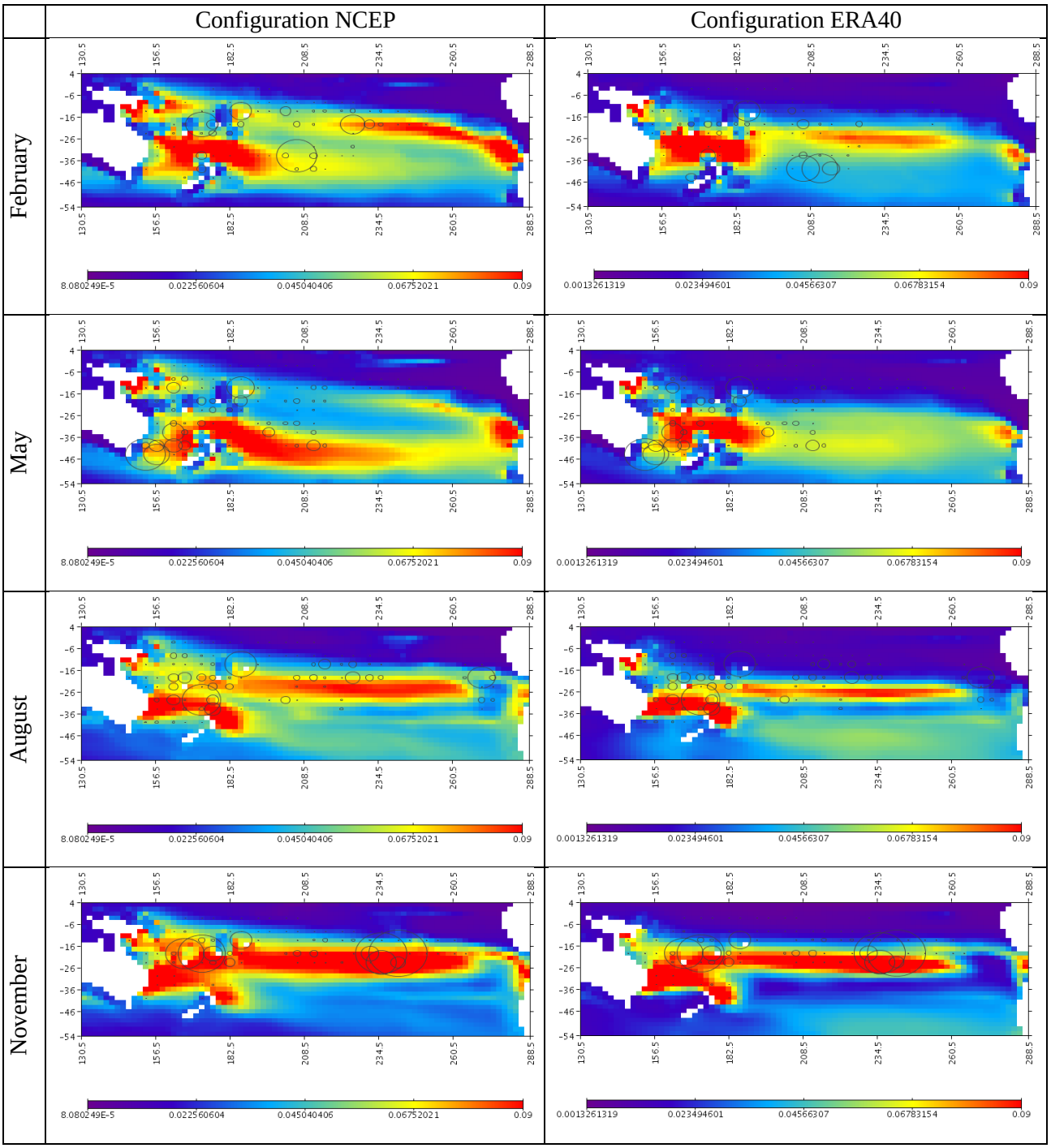

Figure 11. Characteristic seasonal migrations of adult albacore predicted with NCEP-ORCA2-PISCES and ERA40-ORCA2-PISCES configurations. Maps show adult biomass (in g m^{-2}) of albacore in 1999, i.e., the last year taken for the optimization experiments, with superimposed observed catch proportional to circles.

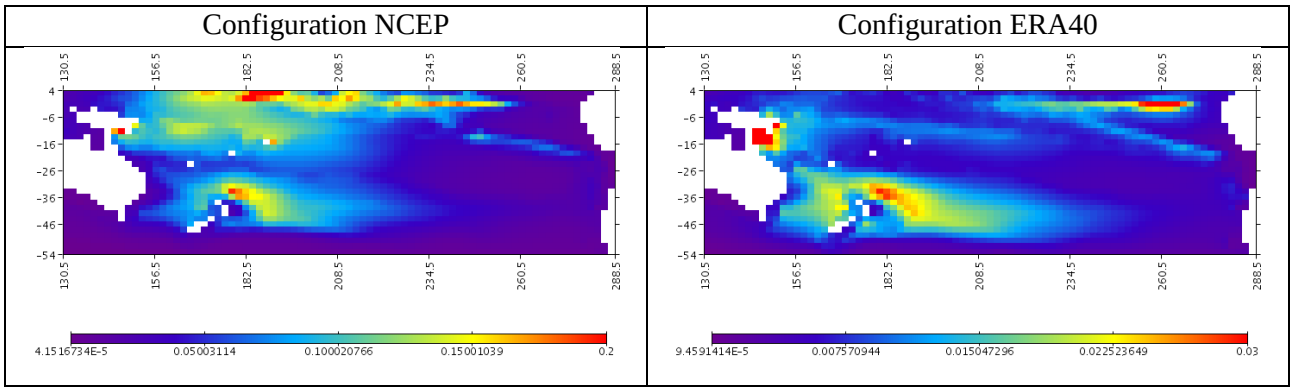

Figure 12. Biomass distribution of young albacore tuna in December 1999

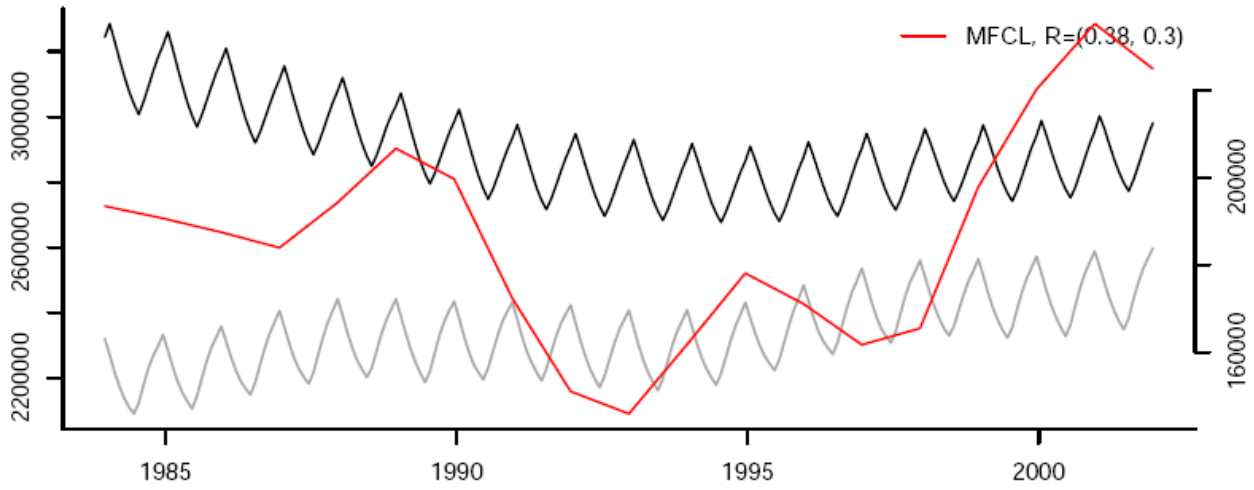

Figure 13. Comparison between adult biomass (in metric tonnes) predicted by MULTIFAN-FCL (red, right axis) and SEAPODYM -ERA40 (black) and SEAPODYM-NCEP (gray) model configurations.

Conclusion and further developments

The optimization approach in SEAPODYM and the evaluation using historical fishing data are key steps to give confidence in the model estimates. While there is a small number of parameters to calibrate, achieving a plausible set of biological parameters remains nevertheless a difficult task requiring a large number of simulations. The quantity, quality and diversity of data are key criteria to quickly achieve a good parameterization. The bigeye application was likely the easiest to perform as the information for this species is covering many fisheries, at different life stages and all over the Pacific Basin from equator to temperate regions. Optimization experiments for this species quickly provided reasonable values of the biological parameters fully consistent with existing knowledge.

We can expect similarly a substantial improvement in the future experiments for yellowfin tuna while including more detailed data, especially for the EPO fisheries. Enhanced environmental forcing data sets should facilitate also this goal. More realistic environmental fields at higher resolution are especially important for skipjack application since this species has fast spatial population dynamics dominated by ENSO variability. We are therefore exploring the possibility of using much more realistic physical forcing based on ocean model assimilating satellite and in situ data (Fig 14). However, due to the requirements for assimilation, this sort of reanalysis is limited to the last 15 years. This may be sufficient for optimization experiments for skipjack (and yellowfin?) but likely not for longer living species (bigeye and albacore).
Finally, running the model with both north and south Pacific albacore should bring more information for the parameter calibration, especially due to the opposite seasonal pattern in the cycle of these species.

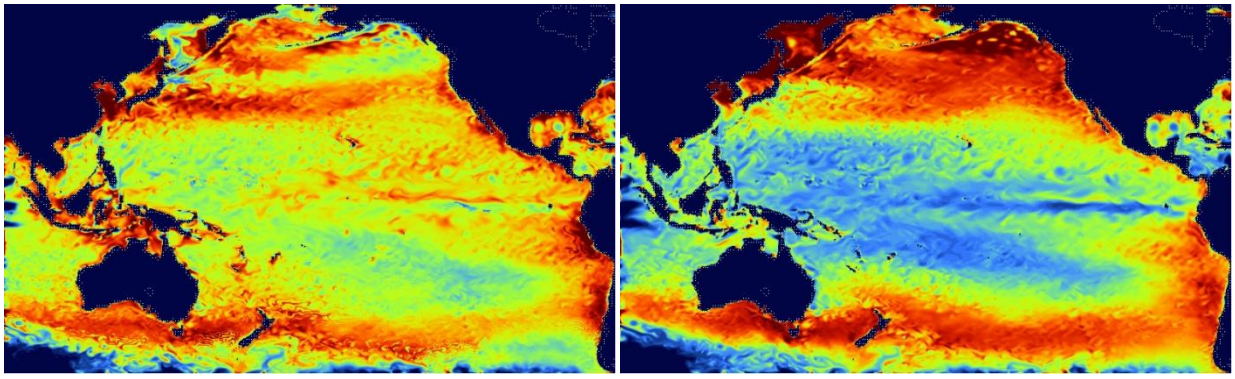

Fig. 14. Snapshots of predicted production (left) and biomass (right) of epipelagic component of micronekton at ¼ deg x 6 day resolution, using MERCATOR temperature and currents and satellite derived primary production. Mesoscale features are clearly visible.

Another way to enhance the skills of the model for predicting the dynamics of the species is to include tagging data in the optimization process. A separate simplified version of the model using conventional tagging data has been tested (Fig 15a) for skipjack and provided close results to those obtained with John Sibert's model (Sibert et al., 1999). The next key step will be to integrate this development with the full population dynamics model. Another challenging development is to also include archival tagging data. A preliminary work for this task is carried out under an ongoing project devoted to Atlantic bluefin tuna (LPRC project: "Parameter estimation of habitat driven spatial dynamics of Atlantic bluefin tuna with tagging data", Lehodey et al. 2009, Fig. 15b).

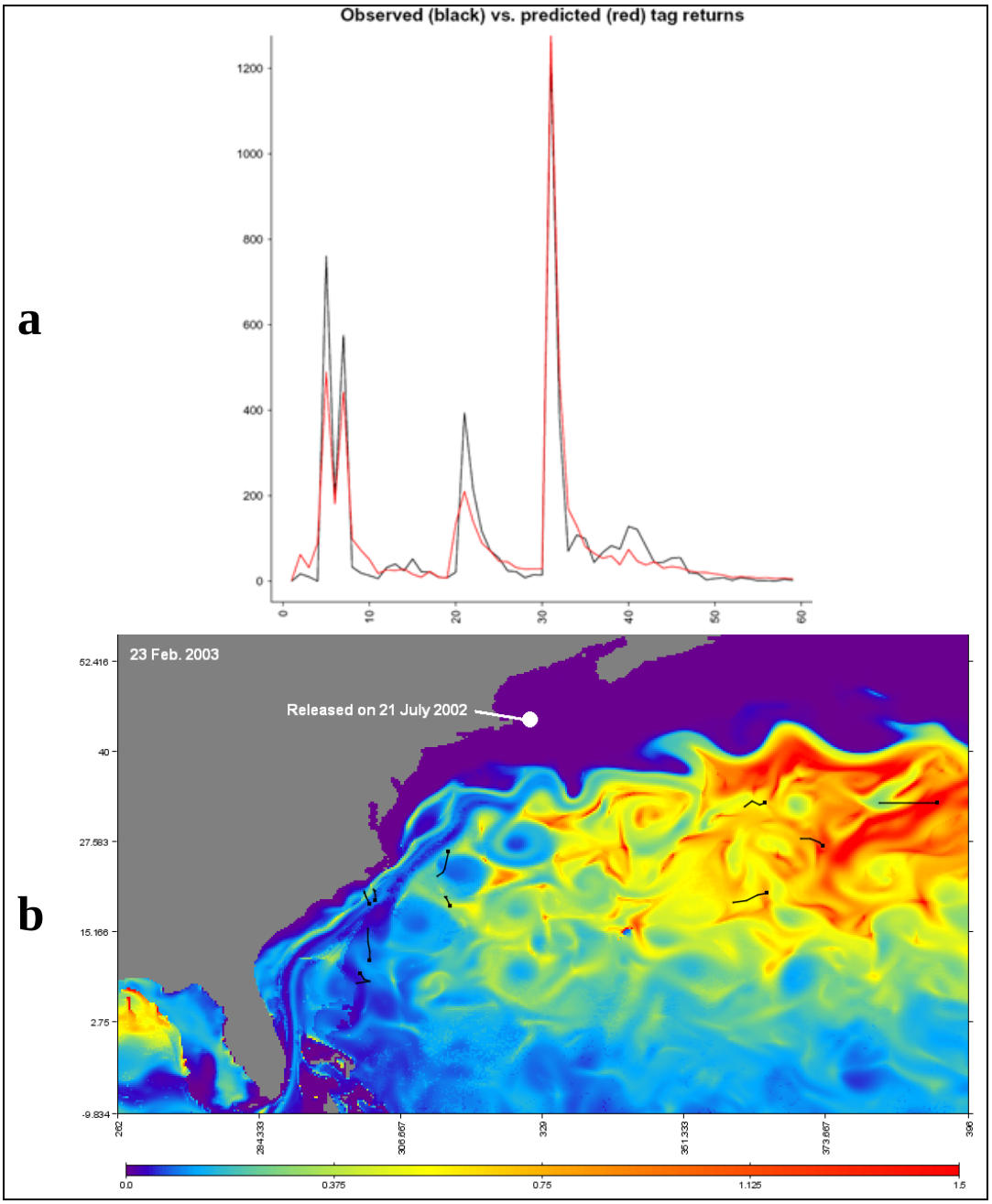

Figure 15: Using tagging data in SEAPODYM. Top: Predicted versus observed conventional tag returns from the skipjack SPC large scale tagging experiment (1977-82) using simplified one-cohort application. Bottom: Snapshot of individual Atlantic bluefin tracks (black lines) deduced from archival satellite tags superimposed on predicted habitat in the North-western Atlantic (spatial resolution of $1/12^{th}$ deg).

Our immediate objective for the coming months under the OFP SciFish project is to achieve optimization experiments for the four pacific tuna species using the best present environmental configuration, and to compare the results to those from MULTIFAN-CL. Using this parameterization, simulations will be

conducted to update a study on the impact of implementing no-fishing areas in enclaves of international waters between Pacific States EEZs, under different scenarios of redistribution of fishing effort.

With the support of the NMFS/NOAA Pacific Islands Fisheries Science Center in Hawaii, a study has been initiated to apply the model SEAPODYM to Pacific swordfish, in collaboration with the OFP. As for tuna species the objective is to let the model to estimate the parameterization for the habitats and dynamics of swordfish population(s) at the basin scale, without defining *a priori* several sub-populations. Thus, as for tuna it is critical to build up the most complete and accurate fishing database (catch, effort and size frequency) for swordfish at the Pacific basin-scale. The support of both IATTC and WCPFC is required here to obtain official agreement to complete the fishing data set we need to develop an application of the model SEAPODYM for swordfish at the Pacific basin-scale.

The achievement of a first analysis of the impact of Climate Change on Pacific skipjack under B2 and A1 IPCC scenarios is also a priority. For such studies on the impact of Climate Warming on tuna populations, it is really critical to validate the simulations results by all possible means. Following the approach used for Earth Climate models, ensemble simulation experiments using different forcings and models have demonstrated considerable advantages. For tuna, it is possible also to test the validity of the mechanisms of the model by applying the optimal parameterization achieved in one ocean to the other oceans. Such comparative analyses have been proposed and supported through a PFRP project and the international CLIOTOP programme, but they require the definition of a public global tuna fishing dataset accessible by the research community. Though such data sets exist for the Indian and Atlantic Ocean, it is still not the case for the Pacific. It becomes urgent to define such a dataset to promote international research collaboration on the issue of climate change that has very likely already altered the oceanic environment of tuna during the last two decades.

Acknowledgments

We would like to acknowledge John Hampton, Tim Lawson and Peter Williams (SPC) and Michael Hinton (IATTC) for discussing fisheries definition, and preparing and supplying catch and size composition data. This work was funded by the European-funded Pacific Regional SciFish Programme of the Oceanic Fisheries Programme of the Secretariat of the Pacific Community, by the Cooperative Agreement NA17RJ1230 between the Joint Institute for Marine and Atmospheric Research (JIMAR) and the National Oceanic and Atmospheric Administration (NOAA), and by the Marine Ecosystems Modeling and Monitoring by Satellites section in CLS, France. Views expressed in the paper do not necessarily represent the views of these agencies or organizations.

References

Aumont, O., L. Bopp, 2006. Globalizing results from ocean in situ iron fertilization studies, Global Biogeochemical Cycles, 20.

Aumont, O.; Maier-Reimer, E.; Blain, S.; Monfray, P. (2003). An ecosystem model of the global ocean including Fe, Si, P colimitations. Global Biogeochemical Cycles, 17(2), DOI 10.1029/2001GB001745

Bopp L, Aumont O, Cadule P, S. Alvain and M. Gehlen (2005). Response of diatoms distribution to global warming and potential implications: A global model study, Geophysical Research Letters, 32 (19).

Chen, D., L.M. Rothstein and A.J. Busalacchi, 1994. A hybrid vertical mixing scheme and its application to tropical ocean models. J. Phys. Oceanog., 24: 2156-2179.

Fournier, D.A., Hampton, J., and Sibert, J.R. 1998. MULTIFAN-CL: a length-based, age-structured model for fisheries stock assessment, with appliacation to South Pacific albacore, Thunnus alalunga. Can. J. Fish. Aqu. Sci., 55: 2105-2116.

Gent, P. R., and M. A. Cane, 1989: A reduced gravity, primitive equation model of the upper equatorial ocean. Comp. Phys., 81, 444-480.

Gorgues, T., C. Menkes, O. Aumont, J. Vialard, Y. Dandonneau, and L. Bopp (2005), Biogeochemical impact of tropical instability waves in the equatorial Pacific, Geophys. Res. Lett., 32, L24615, doi:10.1029/2005GL024110.

Hampton, J., Langley, A., & Kleiber, P. (2006). Stock assessment of bigeye tuna in the western and central Pacific Ocean, including an analysis of management options. 2nd Meeting of the Scientific Committee of the Western and Central Pacific Fisheries Commission. Manila, Philippines, 7-18 August 2006, WCPFC-SC2-SA WP-2, 103 pp

Hoyle,S., A. Langley,and J. Hampton (2008). Stock assessment of Albacore tuna in the south Pacific Ocean. 4th Meeting of the Scientific Committee of the Western and Central Pacific Fisheries Commission. Port Moresby, Papua New Guinea, 11-22 August 2008, WCPFC-SC4-2008/SA-WP-8, 126 pp

Kalnay, E., Kanamitsu, M., Kistler, R., Collins, W., Deaven, D., Gandin, L., Iredell, M., Saha, S., White, G., Woollen, J., Zhu, Y., Leetmaa, A., Reynolds, B., Chelliah, M., Ebisuzaki, W., Higgins, W., Janowiak, J., Mo, K.C., Ropelewski, C., Wang, J., Jenne, R., Joseph, D. (1996). The NCEP/NCAR 40-Year Reanalysis Project. Bulletin of the American Meteorological Society: **77**, pp. 437-472.

Langley, A., Hampton, J., Kleiber, P., Hoyle S. (2007). Stock assessment of yellowfin tuna in the western and central Pacific Ocean, including an analysis of management options. 3rd regular session of the Scientific Committee of the Western Central Pacific Fisheries Commission, 13-24 August 2007 Honolulu, United States of AmericaWCPFC–SC3 SA WP–1: 120 pp.

Lehodey P., & Senina I.. (2009). A USER MANUAL FOR SEAPODYM VERSION 2.0: application with data assimilation (draft version)., 5th Regular session of the Scientific Committee of the Western Central Pacific Fisheries Commission, 10-21 August 2007 Port Vila, Vanuatu. WCPFC–SC5 EB IP–13.

Lehodey P., Senina I., & Murtugudde R. (2008). A Spatial Ecosystem And Populations Dynamics Model (SEAPODYM) - Modelling of tuna and tuna-like populations. *Progress in Oceanography*, **78**: 304-318.

Lehodey P., Senina, I., Royer, F., Jouanno, J., Sibert, J., Lutcavage, M., Gaspar, P., & Fromentin, J-M. (2009). Parameter estimation of habitat driven spatial dynamics of Atlantic bluefin tuna with tagging data. GLOBEC Newsletter 15 (1): 17-19

Lehodey P., Murtugudde R., Senina I. (*accepted*). Bridging the gap from ocean models to population dynamics of large marine predators: a model of mid-trophic functional groups. *Progress in Oceanography*. Special issue of the EUR-OCEANS conference "Parameterisation of Trophic Interactions in Ecosystem Modelling", 20-23 March 2007, Cadiz, Spain.

Leonard, C.L., C.R. McClain, R. Murtugudde, E. E. Hofmann, and L.W. Harding, Jr., 1999. An iron-based ecosystem model of the central equatorial Pacific. *J. Geophys. Res*. **104**: 1325-1341

Moore, J.K., Doney, S.C., Lindsay, K., (2004). Upper ocean ecosystem dynamics and iron cycling in a global three-dimensional model. *Global Biogeochem. Cycles*, **18** doi:10.1029/2004GB002220

Murtugudde, R., R. Seager and A. Busalacchi, 1996. Simulation of the tropical oceans with an ocean GCM coupled to an atmospheric mixed layer model. *J. Clim*. **9**: 1795-1815.

Lehodey and Senina (2009). *A User manual for SEAPODYM Version 2.0: application with data assimilation. Information paper?: 79 pp.*

Senina I., Sibert J., & Lehodey P. (2008). Parameter estimation for basin-scale ecosystem-linked population models of large pelagic predators: application to skipjack tuna. *Progress in Oceanography*, **78**: 319-335.

Sibert, J., & Hampton, J. (2003). Mobility of tropical tunas and the implications for fishery management. *Marine Policy* **27**: 87-95.

Sibert, J., Hampton, J., Kleiber, P., Maunder, M. 2006. Biomass, Size, and Trophic Status of Top Predators in the Pacific Ocean. *Science* **314**: 1773-1776.

Six, K. D., and E. Maier-Reimer (1996), Effects of plankton dynamics on seasonal carbon fluxes in an ocean general circulation model, Global Biogeochem. Cycles, 10, 559-583.

Uppala, S.M., Kållberg, P.W., Simmons, A.J., Andrae, U., da Costa Bechtold, V., Fiorino, M., Gibson, J.K., Haseler, J., Hernandez, A., Kelly, G.A., Li, X., Onogi, K., Saarinen, S., Sokka, N., Allan, R.P., Andersson, E., Arpe, K., Balmaseda, M.A., Beljaars, A.C.M., van de Berg, L., Bidlot, J., Bormann, N., Caires, S., Chevallier, F., Dethof, A., Dragosavac, M., Fisher, M., Fuentes, M., Hagemann, S., Hólm, E., Hoskins, B.J., Isaksen, L., Janssen, P.A.E.M., Jenne, R., McNally, A.P., Mahfouf, J.-F., Morcrette, J.-J., Rayner, N.A., Saunders, R.W., Simon, P., Sterl, A., Trenberth, K.E., Untch, A., Vasiljevic, D., Viterbo, P., and Woollen, J. 2005: The ERA-40 re-analysis. *Quart. J. R. Meteorol. Soc.*, 131, 2961-3012.doi:10.1256/qj.04.176

Yeager, S.G., Shields, C.A., Large, W.G., Hack, J.J., (2006). The low-resolution CCSM3, J. Clim., 19: 2545-2566.

Appendix 1: Major notations and parameterization

For simplicity, notations of species (*sp*), space (*i, j*) and time (*t*) are omitted

Forcing variables		
Z	Vertical layer, total number of layers is 3	
V_z	Vector (u,v) of horizontal currents	nmi· month^{-1}
T_z	Temperature, available for each z	deg C
O_z	Concentration of dissolved oxygen, available for each z	ml.l^{-1}
P	Primary production, vertically integrated	g.m-^{2}.d^{-1}
S_n	Production of immature forage (source for forage) density per unit of time step (six components)	g.m-^{2}
F_n	Biomass of forage populations (six components)	g.m-^{2}
F_p	Biomass of forage potentially feeding on larvae in the surface layer	g.m-^{2}
State variables		
J_a	Density of juvenile age class of predator (tuna) population	g.m-^{2}
N_a	density of adult age class of predator (tuna) population in number	
B_a	biomass of adult age class of predator (tuna) population	g.m-^{2}
R	new recruits to predator (tuna) population	g.m-^{2}
B_{adult}	Total biomass of immature and mature adult predators	g.m-^{2}
Internal variables and parameters		
I_0	Larvae's habitat index (only one cohort in present configuration)	
$I_{1,k}$	Juvenile's habitat index of cohort *k*	
$I_{2,a}$	Adult's habitat index of cohort *a*	
H_S	Spawning habitat index	
$H_{F,a}$	Feeding habitat index of cohort *a*	
$\Theta_{a,n}$	Accessibility coefficient of predator (tuna) cohort *a* to forage component *n*	
$\vartheta_{n,a}$	Accessibility coefficient of predator cohort *a* to forage component *n* relative to all forage components	
D	Day length function of latitude and date	h
G_d	Gradient of day length	h.d^{-1}
G_{max}	Maximum gradient of standardized habitat	
G_x (G_y)	Gradient of habitat index in the x (y) direction	
$D_{a\,max}$	Maximum diffusion coefficient for cohort *a* (at size l_a)	nmi^{2} · month^{-1}
D_a	Diffusion coefficient for cohort *a* (at size l_a)	nmi^{2} · month^{-1}
χ	Taxis coefficient	nmi· d^{-1}
$I_{FR,a}$	Food requirement index of cohort *a*	
F_{Rn}	Total requirement of forage component n	g
ω_n	Mortality of forage component *n* due to all predator cohorts	
M_P	tuna predation mortality	time^{-1}
M_S	tuna senescence mortality	time^{-1}

Pre-defined parameters		unit	SKJ	YFT	BET	SP alb.
	Population structure					
	Number of larvae cohorts (month)		1	1	1	1
	Number of juvenile cohorts (month)		2	2	2	2
	Age at 1st autonomous displacement	month	4	4	4	4
	Number of young cohorts (3 mo; 6 mo; 12 mo)		2 (3 mo)	2 (6 mo)	4 (6 mo)	9 (6 mo)
	Age at 1st maturity	month	9	15	27	57
	Number of adult cohorts (3 mo; 6 mo; 12 mo)		12 (3 mo)	12 (6 mo)	16 (6 mo)	11 (12 mo)
	Growth					
l_a	Predator' size of cohort *a*	cm	*	*	*	*
w_a	Predator' weight of cohort *a*	kg	*	*	*	*
	Food requirement (*optional*)					
r	Daily ration (relative to weight at age)	-	0.10	0.06	0.06	0.05
ρ	Coefficient of the Food requirement index function	-				0.02
	Habitats					
κ	curvature parameter in the function to switch continuously from feeding to spawning habitat	-	1000	1000	1000	1000
$\hat{G}_d$	Threshold in the gradient of day length at which the switch occurs between spawning and feeding habitat	$h.d^{-1}$	0.015	0.010	0.025	0.008

* from independent studies (Langley et al., 2005; Hampton et al., 2006; Langley et al. 2007; Hoyle et al. 2008)

Parameters estimated by the model			unit	SKJ	YFT		BET	SP alb.	
				ESSIC	NCEP	ERA40	ESSIC	NCEP	ERA40
		Habitats							
1	T_s	Optimum of the spawning temperature function	^oC	30.47	25.98	26.53	26.2	28.9	25.56
2	σ_s	Std. Err. of the spawning temperature function	^oC	3.5*	3*	3.49]	0.82	2.09	0.75*
3	α	Larvae food-predator trade-off coefficient	-	3.67	7.5]	7.15	0.63	5*	5*
4	T_a	Optimum of the adult temperature function at maximum age	^oC	26*	24.07	17	13	17.47	5.65
5	σ_a	Std. Err. of the adult temperature function at maximum age	^oC	2.62	3*	3.99]	2.16	2.23	3.84
6	$\hat{O}$	Oxygen value at Ψ_O =0.5	$ml \cdot l^{-1}$	3.86	0.4*	0.677	0.46	3.93	2.98
7*	γ	Curvature coefficient of the oxygen function	-	-8	0.001*	0.001	0.001*	0.002*	0.016
		Movements							
8	V_M	Maximum sustainable speed	$B.L.\cdot s^{-1}$	1.3	[0.2	0.85*	0.32	1.65*	1.61
9	c	coefficient of diffusion habitat dependence (defines the curvature and the minimum asymptotic value of the function)	-	0.4	0.073	3]	0.22	0.382	1.9
*10***	η	Coefficient of diffusion density dependence (defines the curvature and the maximum asymptotic value of the function)	-	-	-	-	-	-	-
		Larvae recruitment							
11	R_s	Coefficient of larvae recruitment (Beverton-Holt function)	-	0.5*	0.034	0.01	0.0045	0.347	0.002
		Mortality							
12	M_{Pmax}	maximal mortality rate due to predation	mo^{-1}	0.5*	0.2*	0.125*	0.25	0.15*	0.2*
13	M_{Smax}	maximal mortality rate due to senescence	mo^{-1}		0.2*	0.185	0.259	0.0084	0.0095
14*	β_P	slope coefficient in predation mortality	-	0.296	0.105	0.059	0.073	0.024	0.121
15*	β_S	slope coefficient in senescence mortality	-	-0.044	-0.102	-0.147	-0.097	-0.01*	-0.5
16*	$A_{0.5}$	age at which ½ M_{Smax} occurs	Mo	31*	48	40	80.6	96*	58
17**	ε	Coefficient of variability of tuna mortality with food requirement index	-	?	0	0	0	0	0
		Fisheries							
For each fishery	$\boldsymbol{q_f}$	Catchability coeff. of fishery *f*							
	s_f	Target fish length of fishery *f*	cm						
	d_f	Selectivity slope coeff. (if sigmoid function) or width (if Gaussian function) of fishery *f*							

*Fixed; [val = value reaching mimimum boundary value; [val = value reaching maximum boundary value

**Optional (not used in these simulations)

Appendix 2: Definition of fisheries

N	Gear	Region	Description	Nationality	C/E data month/year	Resolution	Size data qtr/year	Resolution
SKIPJACK available data*								
1	PL	15N-45N; 115E-150W	PL West Pac	Japan	1/1972 - 12/2007	5x5	1/1964 - 1/2004	5x5
2	PL	25N-45N; 165E-150W	PL Central Pac	Japan	6/1972 - 11/2007**	5x5	2/1972 - 3/2003**	5x5
3	PS	25N-45N; 140E-165E	PS subtropical fishery	Japan	7/1970 - 9/2007	5x5	2/1974 - 4/2003	5x5
4	LL	20S-25N; 115E-150W	LL exploratory fishery	Japan	6/1950 - 11/2007	5x5	1/1970 - 3/2006	5x5
5	PL	15S-0; 140E-160E	Pole and line	Papua New Guinea	3/1970 - 4/1985	5x5	3/1984 - 4/1985	5x5, 10x20
6	PL	15S-0; 150E-165E	Pole and line	Solomon Islands	6/1971 - 10/2005	5x5	3/1971 - 3/2003	5x5
7	PS	20S-15N; 130E-150W	PS on LOG	All	11/1970 - 4/2008 No Effort	5x5	2/1988 - 1/2007	5x5, 10x20
8	PS	20S-15N; 130E-150W	PS on FAD	All	2/1973 - 4/2008 No Effort	5x5	3/1988 - 3/2007	5x5, 10x20
9	PS	20S-15N; 130E-150W	PS on free school	All	12/1967 - 4/2008 No Effort	5x5	4/1987 - 3/2007	5x5, 10x20
10	DOM	0-15N; 115E-130E	mixed set types	Philippines	1/1970 - 12/2007	5x5	-	-
11	DOM	10S-10N; 120E-130E	mixed set types	Indonesia	1/1970 - 12/2007	5x5	-	-
12	PL	20S-5N; 175E-185E	Pole and Line	Fiji	1/1976 - 11/1998	5x5	4/1991 - 4/1999	5x5, 10x20
13	PS	EPO	PS on Dolphin schools	NA (public data)	10/1959-8/2007	1x1	1/1961 – 4/2005	EPO
14	PS	EPO	PS on Floating objects	NA (public data)	7/1959 – 8/2007	1x1	1/1961 - 4/2005	EPO
15	PS	EPO	PS on free school	NA (public data)	3/1959-8/2007	1x1	1/1961 - 4/2005	EPO

* The current data for WCPO (MFCL 24-regional structure) are available on 5x5degree cells. It would be useful to have data with original (1x1 for most of PL and PS fisheries) resolution.

** Note, that Japan distant water data are available only for a given region while for MFCL regions 1,2,4 data are missing.

N	Gear	Region	Description	Nationality	C/E data month/year	Reso-lution	Size data qtr/year	Reso-lution
YFT and BET available data								
L1	LL	WCPO	Traditional LL fishery targeting BET & YFT	Japan, Korea, Chinese Taipei (DWFN)	6/1950 - 12/2007	5x5	2/1948 – 1/2007	10x20
L2	LL	10S-45N; 110E-140W	Shallow night LL fishery	China, Chinese Taipei	1/1958 - 11/2007	5x5	2/1991 – 2/2007	10x20
L3	LL	40S-10S; 140E-140W	LL fishery targeting South Pac. Albacore	Chinese Taipei, Vanuatu (DWFN), Korea, Japan	7/1952 - 12/2007	5x5	2/1951 – 4/2006	10x20
L4	LL	40S-10S; 145E-140W	Pac. Islands LL targeting South Pac. Albacore	US (Am. Sam), Fiji, Samoa, Tonga, NC, FP, Vanuatu (local)	2/1982 - 12/2007	5x5	3/1991 – 4/2007	10x20
5	LL	20S-15N; 140E-175E	Pac. Islands LL targeting BET & YFT	PNG, Solomons	10/1981 - 5/2007	5x5	2/1996 – 4/2006	10x20
6	LL	40S-10S; 140E-175E	LL Australia East Coast	Australia	10/1985 - 3/2007	5x5	3/1992 – 4/2006	10x20
7	LL	10S-50N; 130E-140W	Hawaii LL	US (Hawaii)	1/1991 - 12/2006	5x5	4/1992 – 3/2006	10x20
8	PS	40S-20N; 114E-140W	PS on drifting FAD & log	All	12/1967 - 2/2008	1x1	2/1988 – 3/2007	5x5
9	PS	40S-20N; 115E-140W	PS on anchored FAD	All	7/1979 - 1/2008	1x1	2/1984 – 2/2007	5x5
10	PS	40S-20N; 114E-140W	PS on free school	All	12/1967 - 1/2008	1x1	3/1984 – 3/2007	5x5
11	PS	10N-50N; 120E-180E	Sub-tropical PS fishery	Japan	7/1970 - 8/2007	1x1	-	-
12	Misc.	10S-15N; 115E-180E	Various domestic fisheries	Philippines	1/1970 - 9/2007	5x5	4/1980 – 4/2007	10x20
13	HL	0N-15N; 115E-130E	Handline fishery	Philippines	1/1970 - 12/2006 Effort missing before 1997	5x5	1993-2007	10x20
14	Misc	10S-10N; 120E-180E	Various domestic fisheries	Indonesia	1/1970 - 1/2007 yes/partially missing	5x5	yft – no data bet - 2006	10x20
15	PL	40S-48N; 115E-140W	Pole-and-line	Japan, Solomon Islands, PNG, Fiji	3/1970 - 12/2006	1x1	yft 4/1977-3/2005 bet 2/1965 – 1/2005	10x20
16	PS	EPO	PS targeting YFT, on Dolphin schools	NA (public data)	1/1959 – 8/2007	1x1	1/1961 – 4/2004	EPO
17	PS	EPO	PS targeting YFT,	NA (public	2/1959 –	1x1	1/1961 –	EPO

N	Gear	Region	Description	Nationality	C/E data month/year	Reso-lution	Size data qtr/year	Reso-lution
			on Floating objects	data)	8/2007		4/2004	
18	PS	EPO	PS targeting YFT, Not associated	NA (public data)	1/1959 – 8/2007	1x1	1/1961 – 4/2004	EPO
19	LL	10N-50N; 150W-90W	Traditional LL targeting BET & YFT	Japan, Korea, Chinese Taipei	11/1954 – 6/2006	5x5	1/1965 – 4/2003	= reg
20	LL	40S-10N; 150W-70W	Traditional LL targeting BET & YFT	Japan, Korea, Chinese Taipei	10/1954 – 7/2006	5x5	4/1954 – 4/2003	= reg

N NCEP ERA40	**Gear**	**Region**	**Description**	**Nationality**	**C/E data month/year**	**Reso-lution**	**Size data qtr/year**	**Reso-lution**
ALBACORE available data								
L1 L1	LL	50S-25S; 140E-110W	JP, JPDW	Japan high latitude	1/1952-12/2006	5x5	3/1964-3/2005	10x20
L1 L12	LL	25S-0; 140E-110W	JP, JPDW	Japan low latitude	1/1952-12/2006	5x5	3/1964-3/2005	10x20
L2 L2	LL	50S-0; 140E-110W		Korea	3/1962-12/2008	5x5	1/1966-2/2006	5x5
L3 L3	LL	50S-0; 140E-110W	Distant-water fleet	Chinese Taipei	7/1964-12/2008	5x5	3/1964-2/2007	5x5; 10x20
L4	LL	50S-10S; 140E-175E	LL targeting Alb	Australia	3/1985-12/2007	5x5	2/2002-2/2007	5x5; 10x20
L5 L5	LL	25S-0; 150E-180E	LL targeting Alb	New Caledonia	11/1983-12/2007	5x5	1/1993-4/2007	5x5; 10x20
L6 L6	LL	50S-0; 140E-180W	LL targeting Alb	Other	11/1957-12/2008	5x5	3/1963-3/2005	5x5; 10x20
L7	LL	50S-25S; 145E-180E	LL targeting Alb	New Zealand	8/1989-12/2007	5x5	2/1992-4/2006	5x5; 10x20
L5	LL	25S-0; 150E-180E	LL targeting Alb	Fiji	8/1989-12/2007	5x5	3/1992-3/2007	5x5; 10x20
L5 L11	LL	25S-0; 180E-155W	LL targeting Alb	American Samoa, Samoa	1/1993-5/2008	5x5	1/1998-3/2007	5x5; 10x20
L5	LL	25S-5S; 180E-140W	LL targeting Alb	Tonga	2/1982-3/2008	5x5	3/1995-242006	5x5; 10x20
L5	LL	25S-0; 180E-110W	LL targeting Alb	French Polynesia	1/1992-5/2007	5x5	2/1991-4/2007	5x5; 10x20
T8	T	50S-25S; 140E-110W	Troll	New Zealand, United States	1/1967-12/2007	5x5	4/1986-2/2006	5x5; 5x10; 10x20
G9	D	45S-25S; 140E-125W	Driftnet	Japan, Chinese Taipei	11/1983-1/1991	5x5	4/1988-1/1990	5x5; 10x20
L10	LL	50S-0; 180-70W	LL targeting Alb	Other	11/1957-12/2008	5x5	3/1963-3/2005	5x5; 10x20

Appendix 3: Yellowfin tuna.

1- Comparison between observed and predicted total catch by fishery

Dotted line: observed catch
Grey line: predicted catch with NCEP configuration
Black line: predicted catch with ERA40 configuration

2- Comparison between observed and predicted size frequency distribution by fishery (all data aggregated in time and space)

Histogram: observed
Dotted Line: predicted with ERA40 configuration
Line with circles: predicted with NCEP

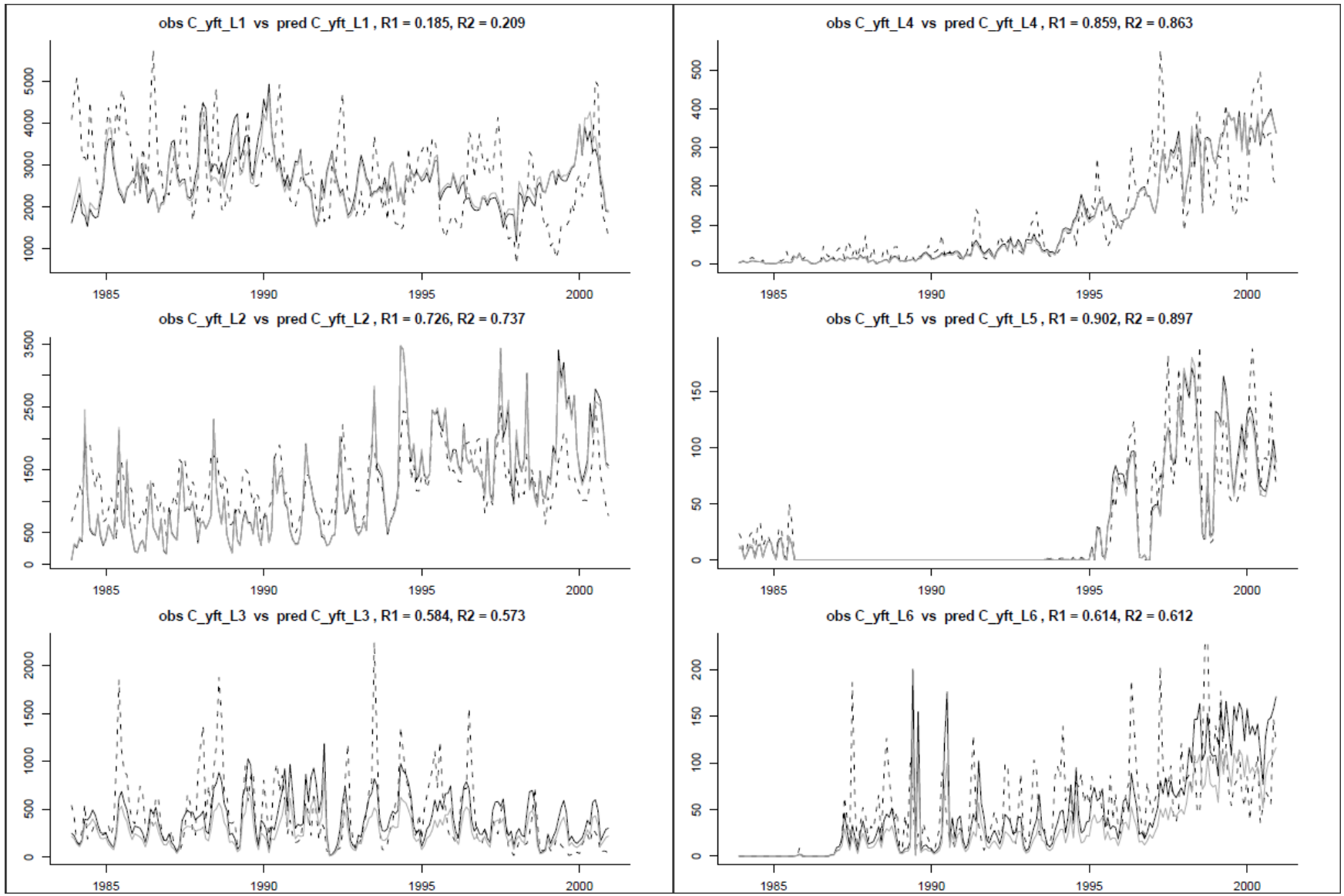
obs C_yft_L1 vs pred C_yft_L1 , R1 = 0.185, R2 = 0.209
obs C_yft_L4 vs pred C_yft_L4 , R1 = 0.859, R2 = 0.863
obs C_yft_L2 vs pred C_yft_L2 , R1 = 0.726, R2 = 0.737
obs C_yft_L5 vs pred C_yft_L5 , R1 = 0.902, R2 = 0.897
obs C_yft_L3 vs pred C_yft_L3 , R1 = 0.584, R2 = 0.573
obs C_yft_L6 vs pred C_yft_L6 , R1 = 0.614, R2 = 0.612
1985
1990
1995
2000

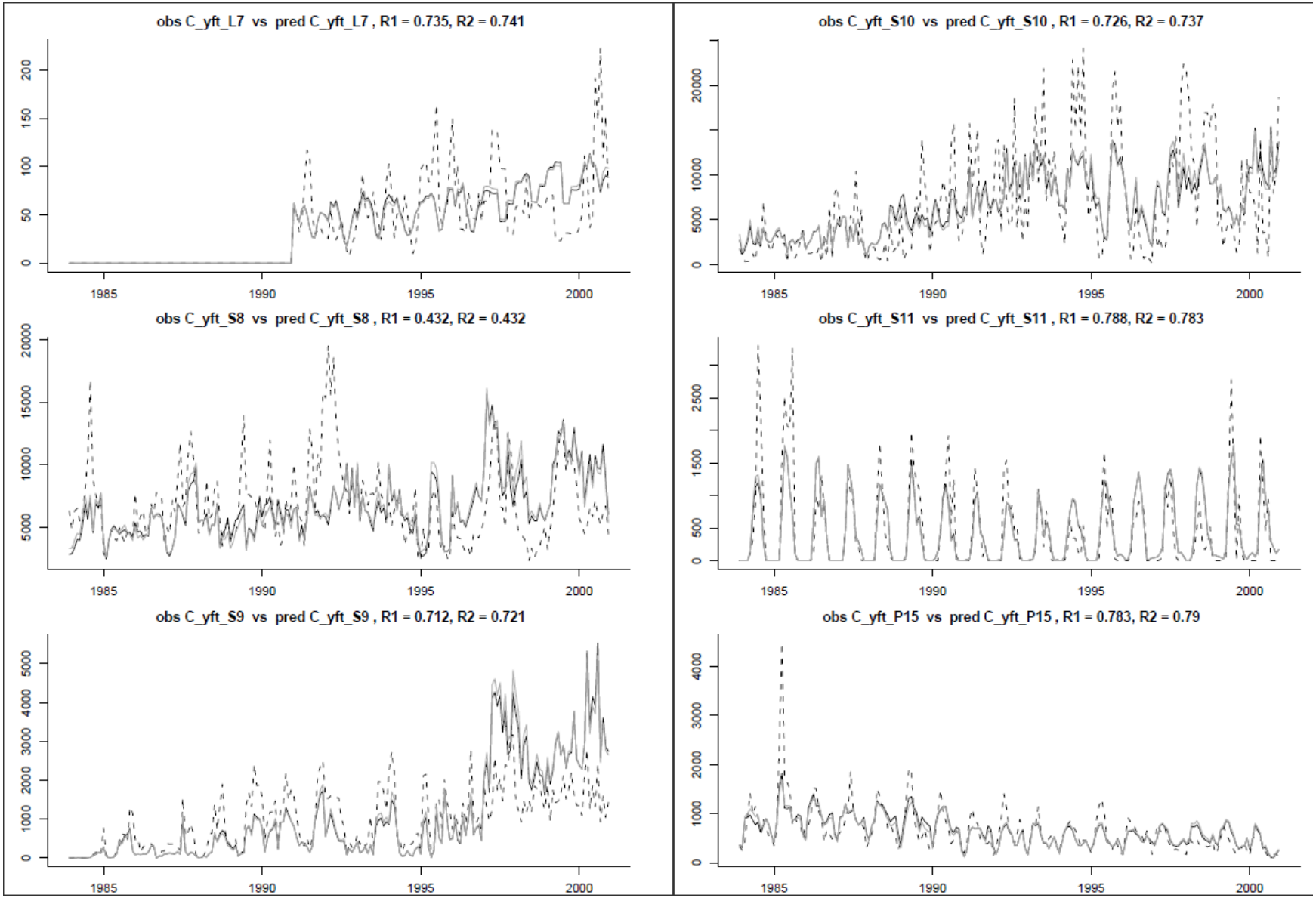
obs C_yft_L7 vs pred C_yft_L7 , R1 = 0.735, R2 = 0.741
obs C_yft_S10 vs pred C_yft_S10 , R1 = 0.726, R2 = 0.737
obs C_yft_S8 vs pred C_yft_S8 , R1 = 0.432, R2 = 0.432
obs C_yft_S11 vs pred C_yft_S11 , R1 = 0.788, R2 = 0.783
obs C_yft_S9 vs pred C_yft_S9 , R1 = 0.712, R2 = 0.721
obs C_yft_P15 vs pred C_yft_P15 , R1 = 0.783, R2 = 0.79
1985
1990
1995
2000

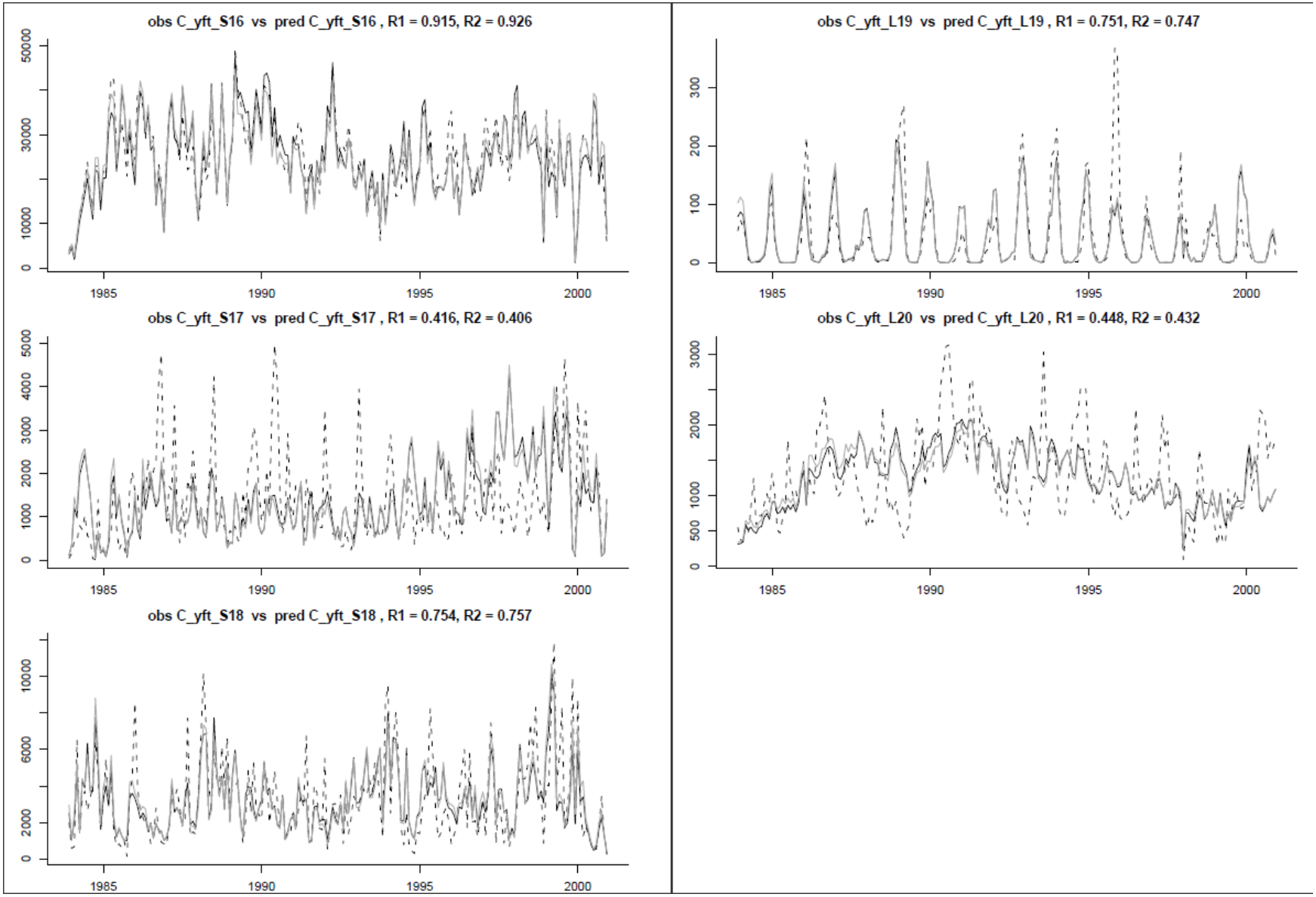
obs C_yft_S16 vs pred C_yft_S16 , R1 = 0.915, R2 = 0.926
obs C_yft_S17 vs pred C_yft_S17 , R1 = 0.416, R2 = 0.406
obs C_yft_S18 vs pred C_yft_S18 , R1 = 0.754, R2 = 0.757
obs C_yft_L19 vs pred C_yft_L19 , R1 = 0.751, R2 = 0.747
obs C_yft_L20 vs pred C_yft_L20 , R1 = 0.448, R2 = 0.432
1985
1990
1995
2000

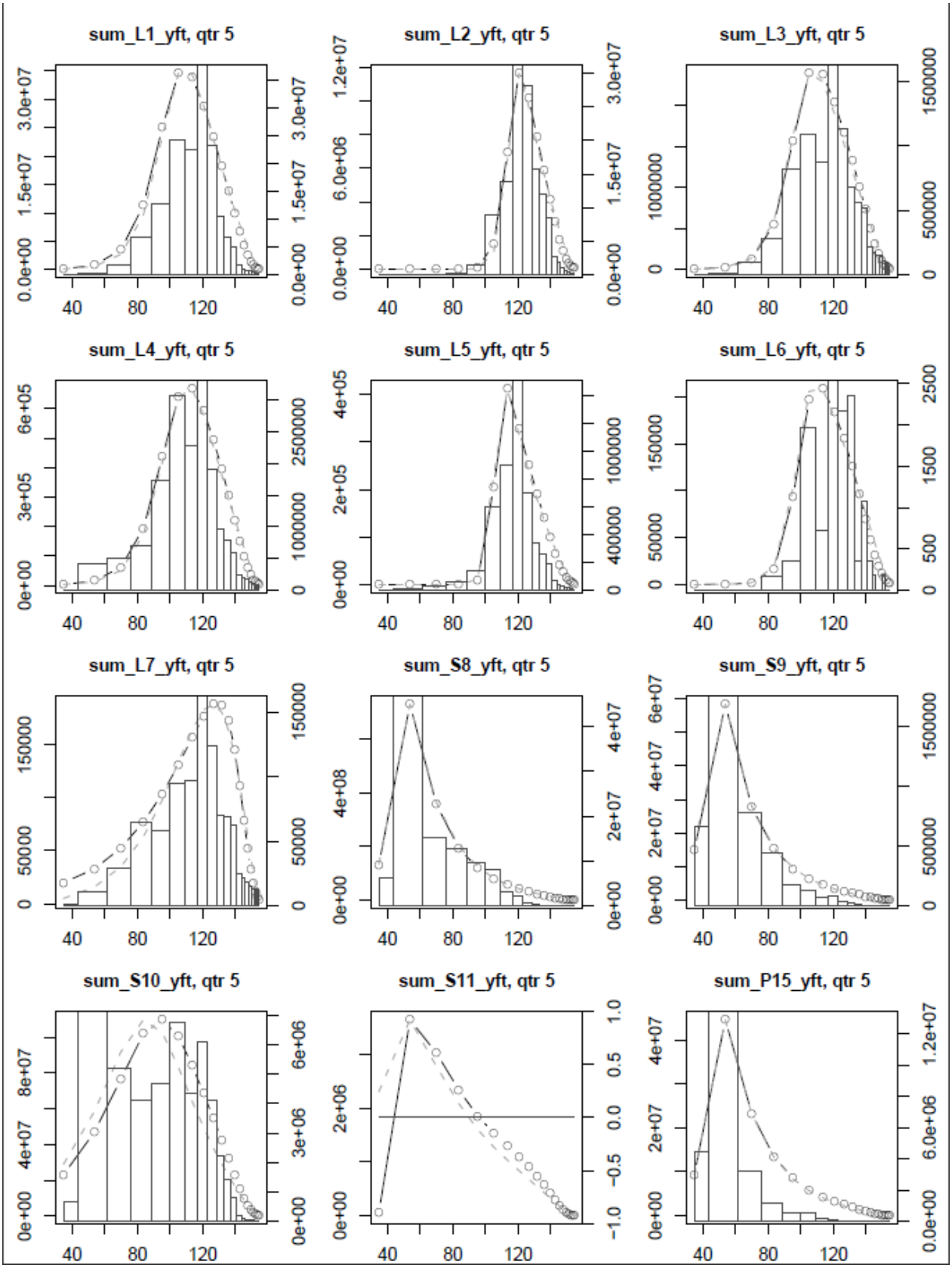
sum_L1_yft, qtr 5
sum_L2_yft, qtr 5
sum_L3_yft, qtr 5
sum_L4_yft, qtr 5
sum_L5_yft, qtr 5
sum_L6_yft, qtr 5
sum_L7_yft, qtr 5
sum_S8_yft, qtr 5
sum_S9_yft, qtr 5
sum_S10_yft, qtr 5
sum_S11_yft, qtr 5
sum_P15_yft, qtr 5

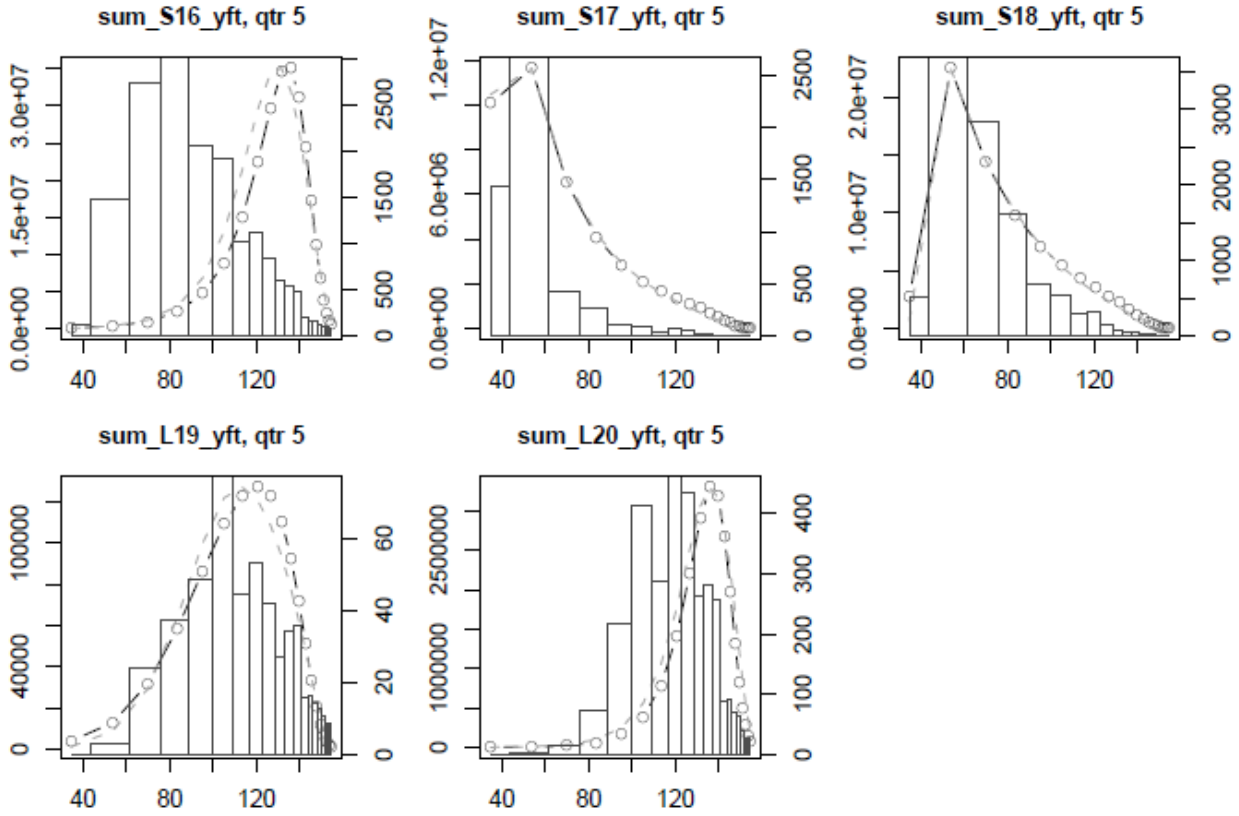
sum_S16_yft, qtr 5
0.0e+00
1.5e+07
3.0e+07
0
500
1500
2500
40
80
120
sum_S17_yft, qtr 5
0.0e+00
6.0e+06
1.2e+07
0
500
1500
2500
40
80
120
sum_S18_yft, qtr 5
0.0e+00
1.0e+07
2.0e+07
0
1000
2000
3000
40
80
120
sum_L19_yft, qtr 5
0
40000
100000
0
20
40
60
40
80
120
sum_L20_yft, qtr 5
0
1000000
2500000
0
100
200
300
400
40
80
120

Appendix 4: Albacore tuna.

1- **Comparison between observed and predicted total catch by fishery**

Dotted line: observed catch
predicted catch with NCEP configuration (page 37-38)
predicted catch with ERA40 configuration (page 40-41)

2- **Comparison between observed and predicted size frequency distribution by fishery (all data aggregated in time and space)**

Histogram: observed
Line with circles: predicted with NCEP (page 39) and ERA40 (page 42)

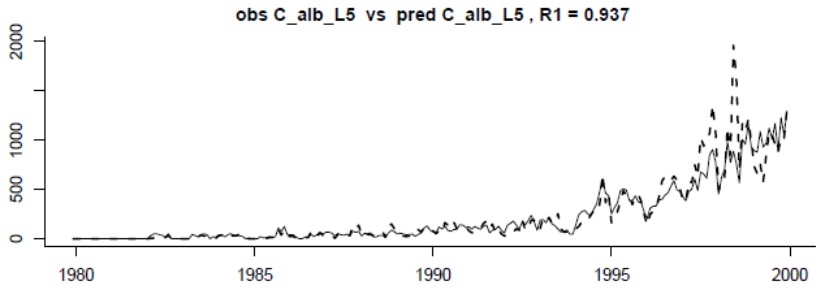
obs C_alb_L5 vs pred C_alb_L5 , R1 = 0.937
0
500
1000
2000
1980
1985
1990
1995
2000

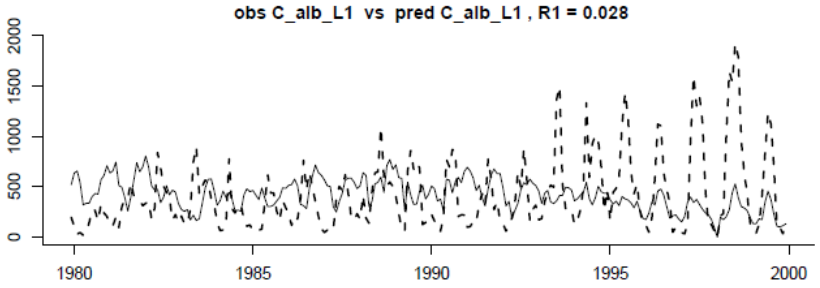
obs C_alb_L1 vs pred C_alb_L1 , R1 = 0.028
0
500
1000
1500
2000
1980
1985
1990
1995
2000

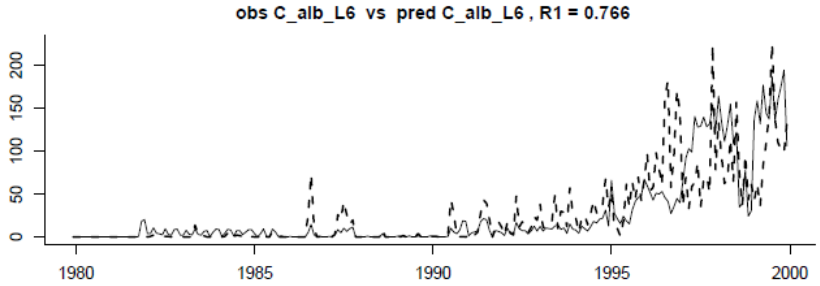
obs C_alb_L6 vs pred C_alb_L6 , R1 = 0.766
0
50
100
150
200
1980
1985
1990
1995
2000

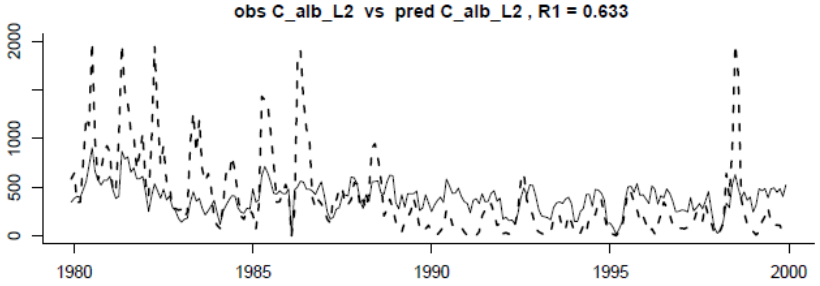
obs C_alb_L2 vs pred C_alb_L2 , R1 = 0.633
0
500
1000
2000
1980
1985
1990
1995
2000

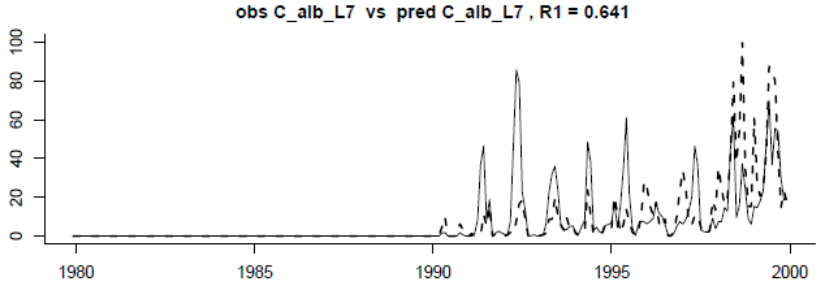
obs C_alb_L7 vs pred C_alb_L7 , R1 = 0.641
0
20
40
60
80
100
1980
1985
1990
1995
2000

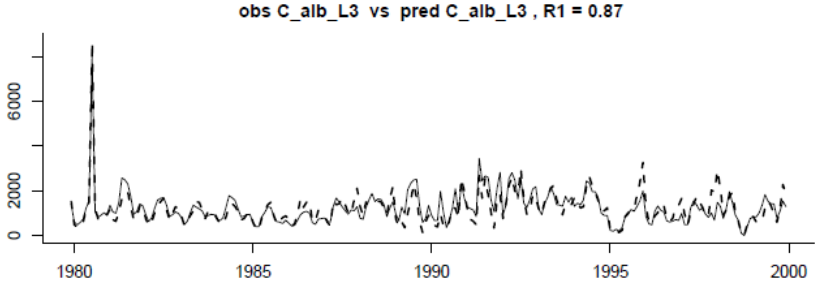
obs C_alb_L3 vs pred C_alb_L3 , R1 = 0.87
0
2000
6000
1980
1985
1990
1995
2000

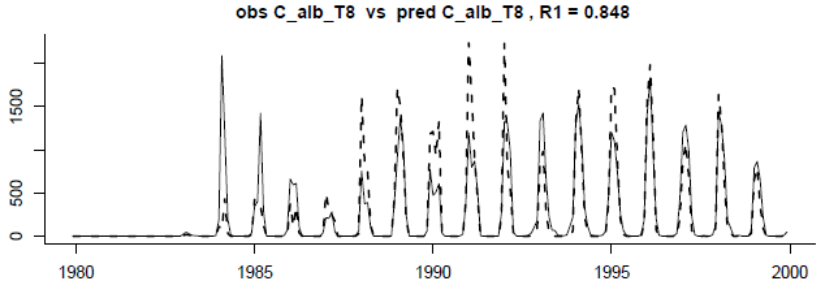
obs C_alb_T8 vs pred C_alb_T8 , R1 = 0.848
0
500
1500
1980
1985
1990
1995
2000

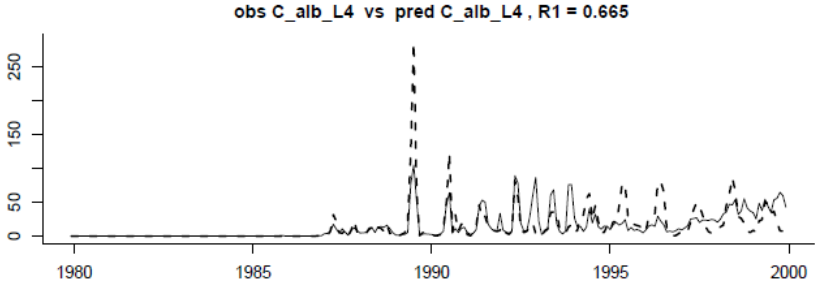
obs C_alb_L4 vs pred C_alb_L4 , R1 = 0.665
0
50
150
250
1980
1985
1990
1995
2000

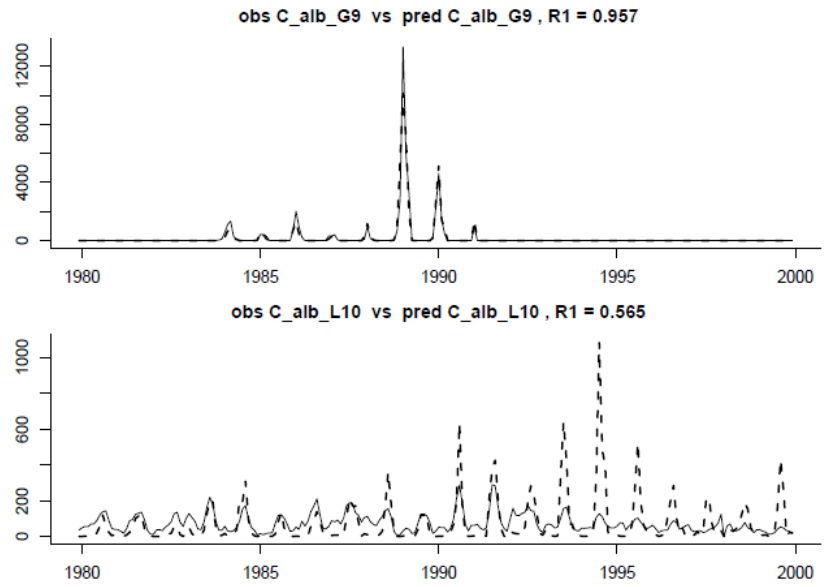
obs C_alb_G9 vs pred C_alb_G9 , R1 = 0.957
0
4000
8000
12000
1980
1985
1990
1995
2000
obs C_alb_L10 vs pred C_alb_L10 , R1 = 0.565
0
200
600
1000
1980
1985
1990
1995
2000

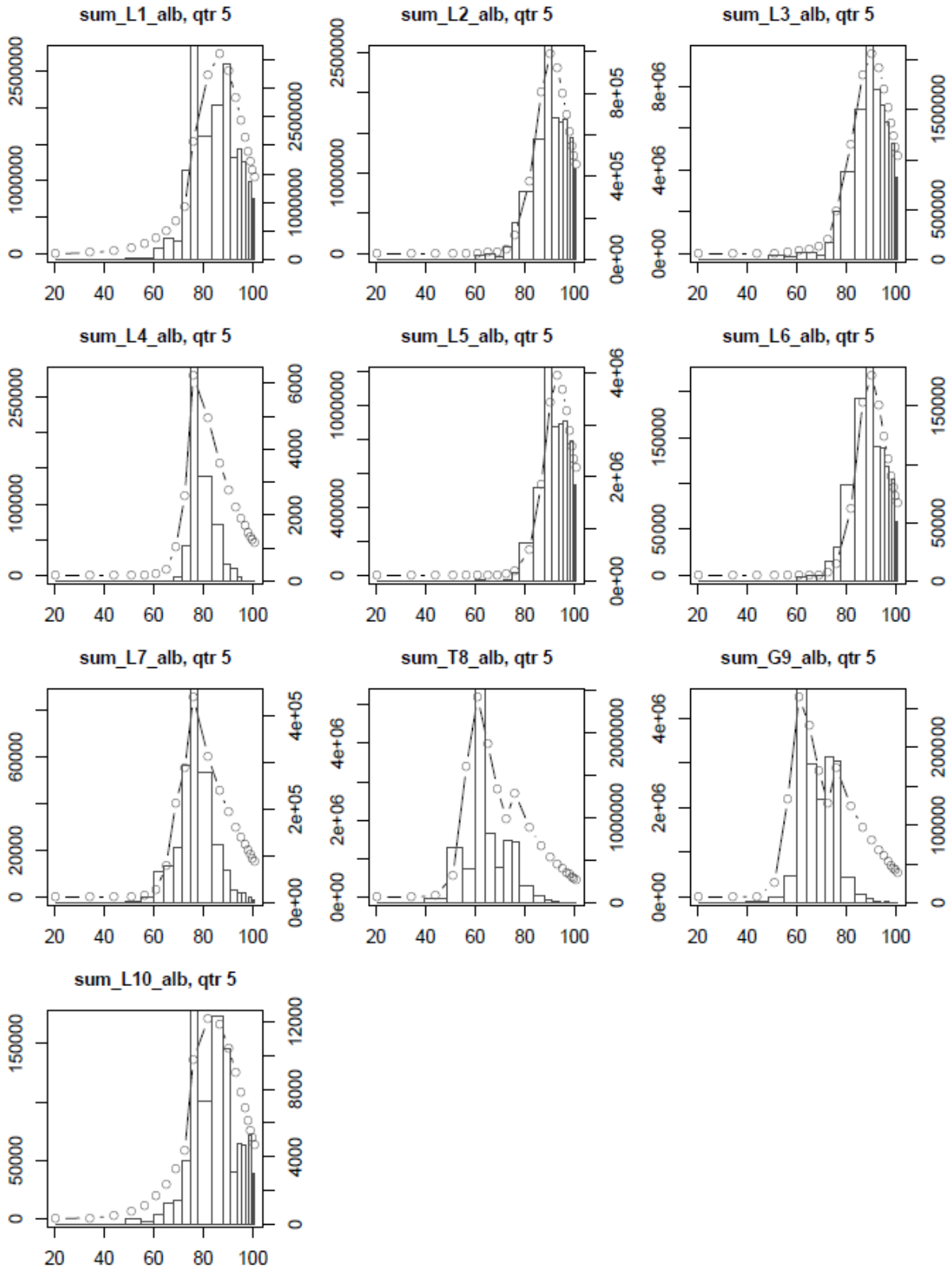
sum_L1_alb, qtr 5
sum_L2_alb, qtr 5
sum_L3_alb, qtr 5
sum_L4_alb, qtr 5
sum_L5_alb, qtr 5
sum_L6_alb, qtr 5
sum_L7_alb, qtr 5
sum_T8_alb, qtr 5
sum_G9_alb, qtr 5
sum_L10_alb, qtr 5

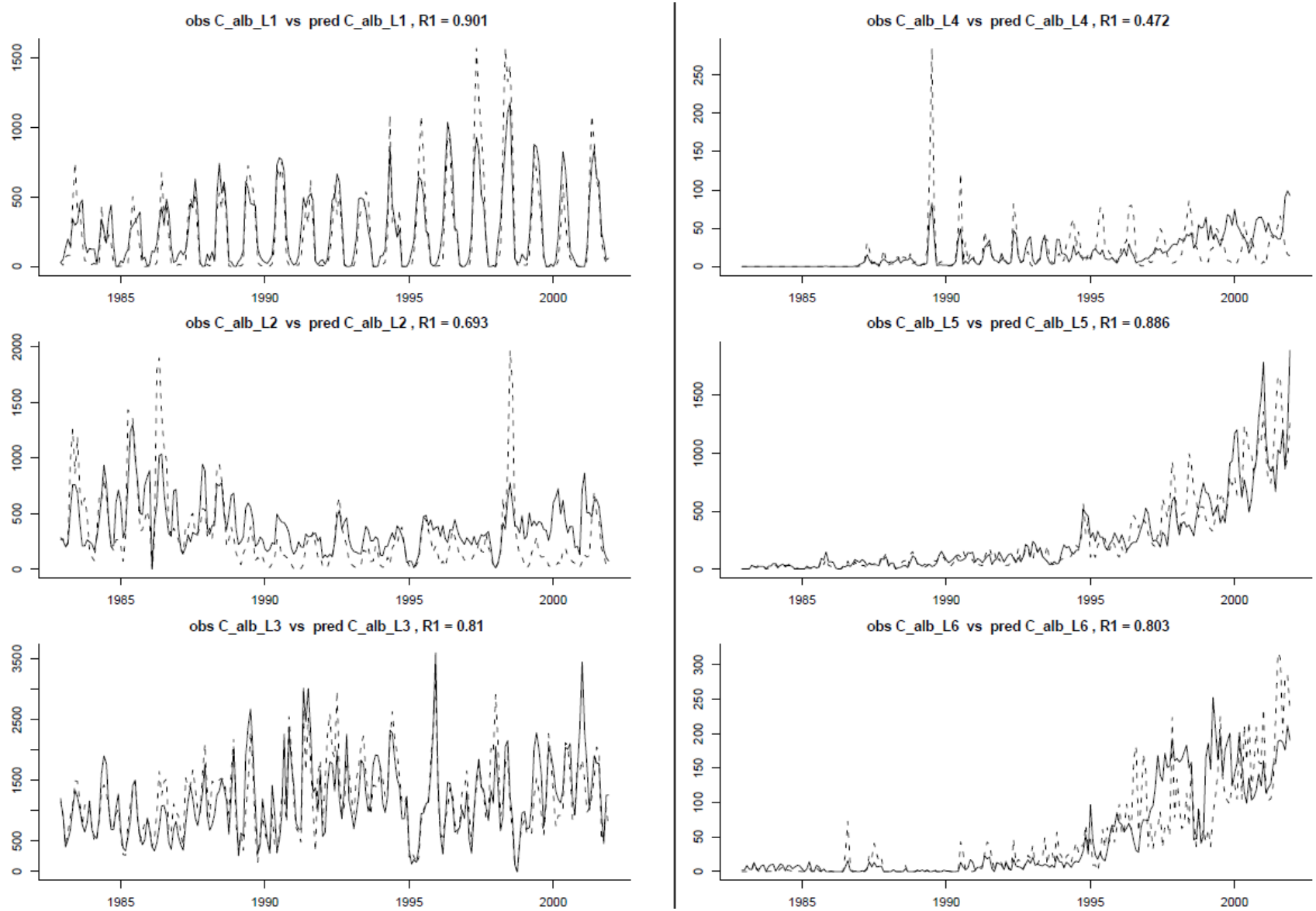
obs C_alb_L1 vs pred C_alb_L1 , R1 = 0.901
obs C_alb_L4 vs pred C_alb_L4 , R1 = 0.472
obs C_alb_L2 vs pred C_alb_L2 , R1 = 0.693
obs C_alb_L5 vs pred C_alb_L5 , R1 = 0.886
obs C_alb_L3 vs pred C_alb_L3 , R1 = 0.81
obs C_alb_L6 vs pred C_alb_L6 , R1 = 0.803
1985
1990
1995
2000

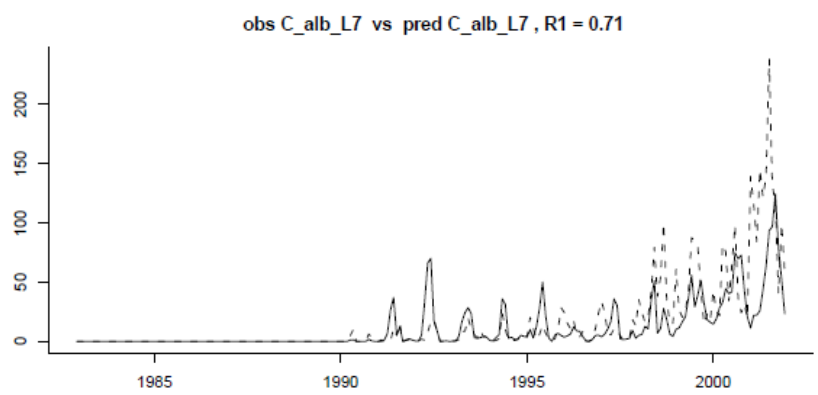
obs C_alb_L7 vs pred C_alb_L7 , R1 = 0.71
0
50
100
150
200
1985
1990
1995
2000

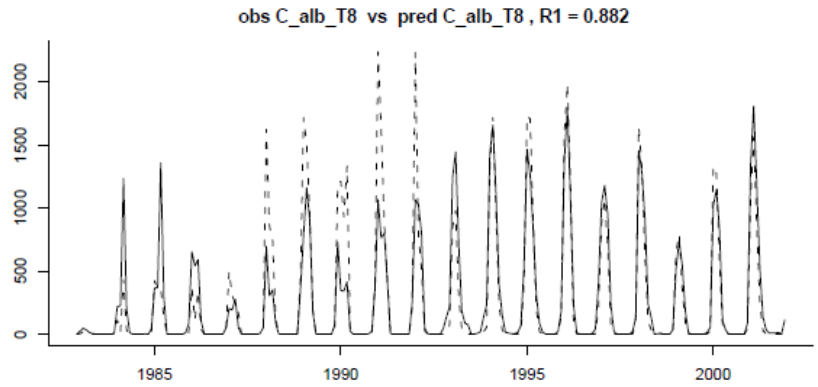
obs C_alb_T8 vs pred C_alb_T8 , R1 = 0.882
0
500
1000
1500
2000
1985
1990
1995
2000

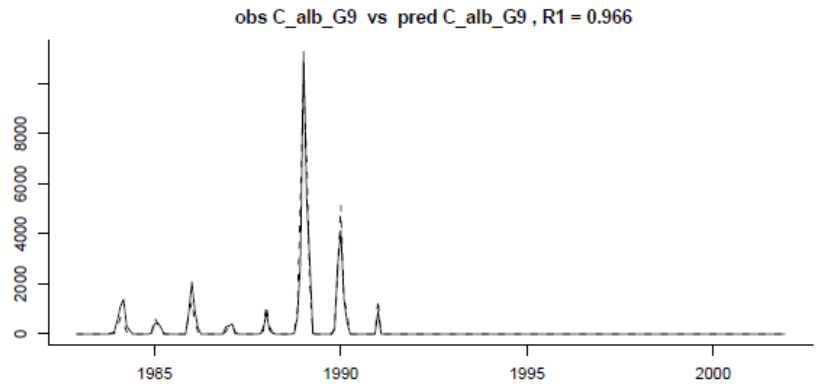
obs C_alb_G9 vs pred C_alb_G9 , R1 = 0.966
0
2000
4000
6000
8000
1985
1990
1995
2000

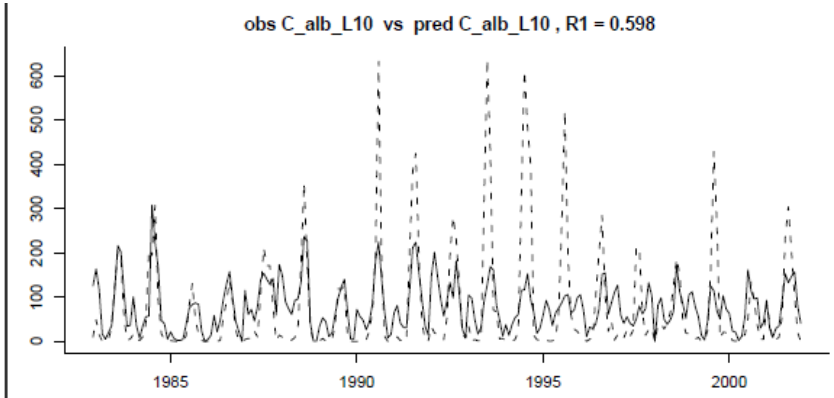
obs C_alb_L10 vs pred C_alb_L10 , R1 = 0.598
0
100
200
300
400
500
600
1985
1990
1995
2000

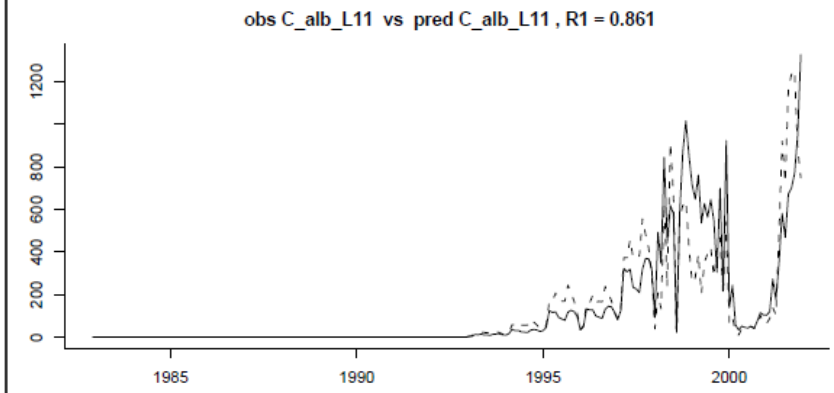
obs C_alb_L11 vs pred C_alb_L11 , R1 = 0.861
0
200
400
600
800
1200
1985
1990
1995
2000

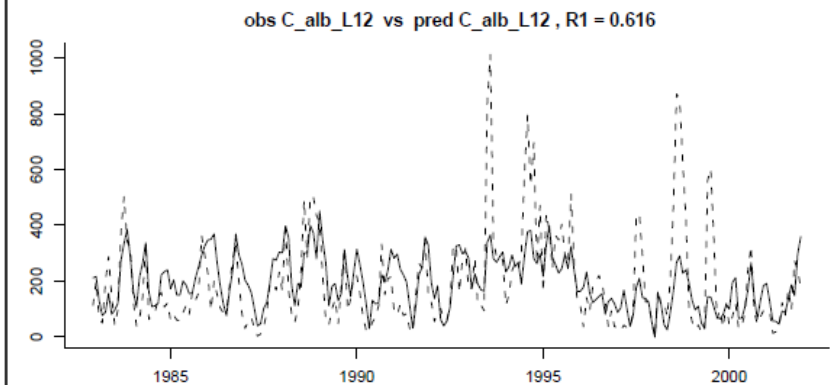
obs C_alb_L12 vs pred C_alb_L12 , R1 = 0.616
0
200
400
600
800
1000
1985
1990
1995
2000

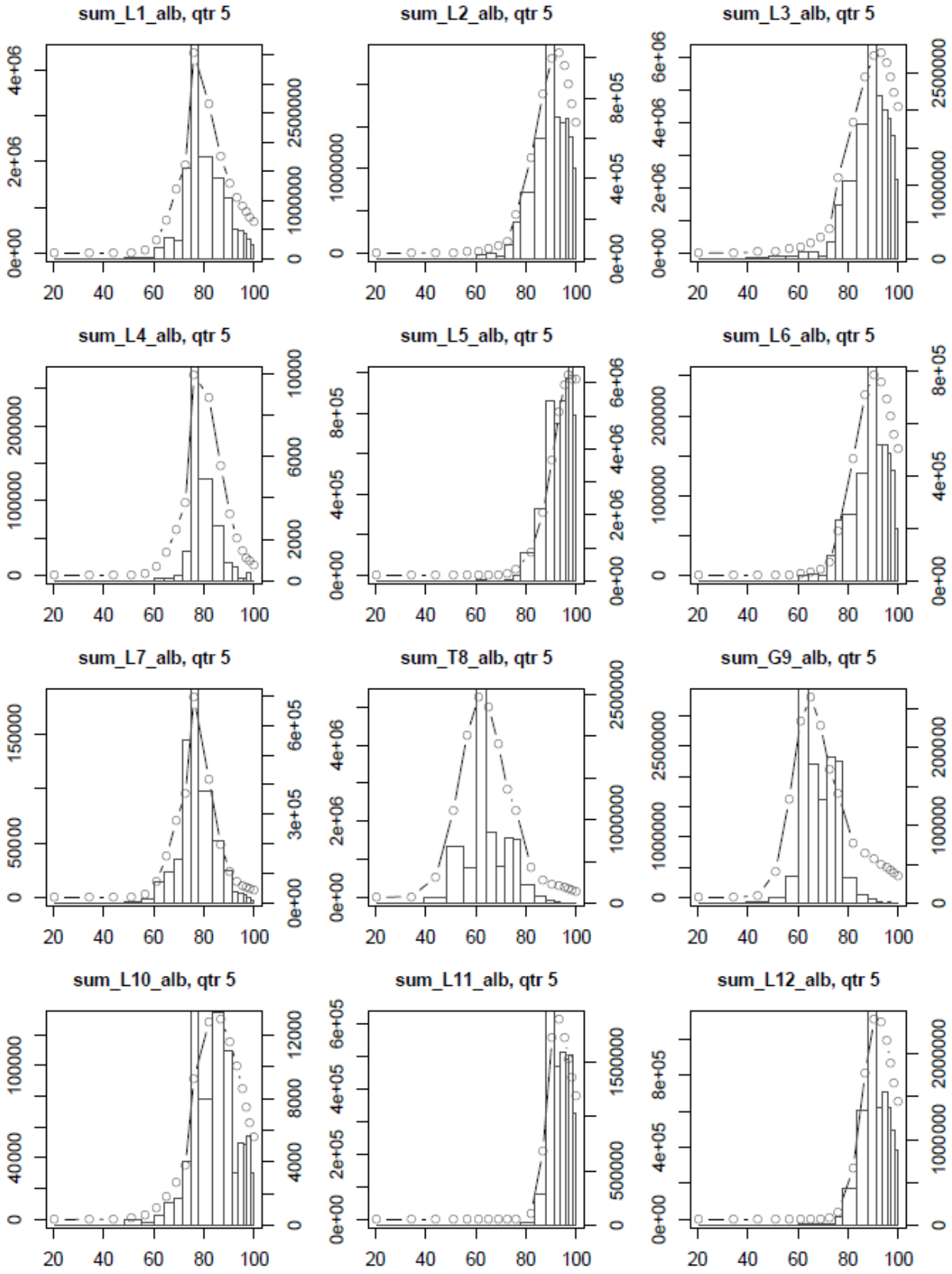
sum_L1_alb, qtr 5
sum_L2_alb, qtr 5
sum_L3_alb, qtr 5
sum_L4_alb, qtr 5
sum_L5_alb, qtr 5
sum_L6_alb, qtr 5
sum_L7_alb, qtr 5
sum_T8_alb, qtr 5
sum_G9_alb, qtr 5
sum_L10_alb, qtr 5
sum_L11_alb, qtr 5
sum_L12_alb, qtr 5